

An encounter-based approach for restricted diffusion with a gradient drift

Denis S Grebenkov* 

Laboratoire de Physique de la Matière Condensée (UMR 7643), CNRS, Ecole Polytechnique, IP Paris, 91120 Palaiseau, France
Institute for Physics and Astronomy, University of Potsdam, 14476 Potsdam-Golm, Germany

E-mail: denis.grebenkov@polytechnique.edu

Received 23 October 2021, revised 3 December 2021

Accepted for publication 8 December 2021

Published 5 January 2022



Abstract

We develop an encounter-based approach for describing restricted diffusion with a gradient drift toward a partially reactive boundary. For this purpose, we introduce an extension of the Dirichlet-to-Neumann operator and use its eigenbasis to derive a spectral decomposition for the full propagator, i.e. the joint probability density function for the particle position and its boundary local time. This is the central quantity that determines various characteristics of diffusion-influenced reactions such as conventional propagators, survival probability, first-passage time distribution, boundary local time distribution, and reaction rate. As an illustration, we investigate the impact of a constant drift onto the boundary local time for restricted diffusion on an interval. More generally, this approach accesses how external forces may influence the statistics of encounters of a diffusing particle with the reactive boundary.

Keywords: boundary local time, reflected Brownian motion, diffusion-influenced reactions, surface reactivity, Robin boundary condition, Heterogeneous catalysis

(Some figures may appear in colour only in the online journal)

1. Introduction

Many transport processes in nature and industry are described by an overdamped Langevin equation for the random position X_t of a particle at time t or, equivalently, by the associated Fokker–Planck equation for the probability density of that position [1–7]. In the presence of restricting boundaries or hindering obstacles, the above descriptions have to be adapted

*Author to whom any correspondence should be addressed.

to account for interactions of the diffusing particle with that boundaries. In physics literature, one usually deals directly with the Fokker–Planck equation by imposing appropriate boundary conditions, while its stochastic counter-part is generally ignored. At the same time, the stochastic differential equation in a confining domain naturally yields additional information on the statistics of encounters of the diffusing particle with the boundary, the so-called boundary local time ℓ_t . In a recent work [8], we investigated ordinary restricted diffusion and showed numerous advantages of using the joint probability density for the pair (\mathbf{X}_t, ℓ_t) to build up a new encounter-based approach to diffusion-influenced reactions and other diffusion-mediated surface phenomena. In particular, surface reactions can be incorporated explicitly via an appropriate stopping condition for the boundary local time. In this way, the bulk dynamics, determined by the pair (\mathbf{X}_t, ℓ_t) in a confining domain with a fully inert reflecting boundary, is disentangled from surface reactions, which are imposed later on. Moreover, this approach allows one to implement new surface reaction mechanisms, far beyond those described by the conventional Robin boundary condition. For instance, one can introduce an encounter-dependent reactivity, in analogy with time-dependent diffusion coefficient for bulk dynamics.

In this paper, we extend the encounter-based approach proposed in [8] to more general diffusion processes with a gradient drift. Section 2 starts by recalling two conventional descriptions of restricted diffusion and discussing the role of the full propagator in the case of ordinary restricted diffusion. After this reminder, we present the main results by introducing an extension of the Dirichlet-to-Neumann operator and using its eigenbasis for deriving a new spectral decomposition for the full propagator, as well as for various characteristics of diffusion-influenced reactions. In section 3, we illustrate our general results in a simple setting of restricted diffusion with a constant drift on an interval (or, equivalently, between parallel planes). The geometric simplicity of this setting allows us to avoid technical issues and to get fully explicit formulas that shed light onto the role of the drift onto boundary encounters. Section 4 presents a critical discussion of the proposed approach and highlights its advantages, drawbacks and limitations, as well as further perspectives.

2. General spectral approach

2.1. Two conventional descriptions

We first recall two conventional descriptions of restricted diffusion in a bounded domain $\Omega \subset \mathbb{R}^d$ with a smooth boundary $\partial\Omega$. On one hand, it can be described by the Skorokhod stochastic differential equation for the random position $\mathbf{X}_t = (X_t^1, \dots, X_t^d)$ of a diffusing particle at time t :

$$d\mathbf{X}_t = \boldsymbol{\mu}(\mathbf{X}_t)dt + \sqrt{2D}d\mathbf{W}_t - \mathbf{n}(\mathbf{X}_t)d\ell_t, \quad \mathbf{X}_0 = \mathbf{x}_0, \quad (1)$$

where \mathbf{x}_0 is the starting point [9–11]. Here the infinitesimal displacement $d\mathbf{X}_t$ of the particle has three contributions: (i) the deterministic part with a drift $\boldsymbol{\mu}(\mathbf{x})$, (ii) random (thermal) fluctuations with the standard Gaussian noises $d\mathbf{W}_t$ whose amplitudes are determined by the diffusion coefficient D , and (iii) reflections from the boundary $\partial\Omega$ along the unit normal vector $-\mathbf{n}(\mathbf{x})$ (oriented inward the domain), whenever the particle hits the boundary. Intuitively, the last term can be understood as an infinitely strong but infinitely short-ranged force that repels the particle from the boundary back to the bulk (see a physical rationale behind this force in SM.I of [8]). Such instant reflections are governed by the boundary local time ℓ_t —a non-decreasing stochastic process (with $\ell_0 = 0$) that increases at each encounter with the boundary (see figure 1). Curiously, the single Skorokhod equation determines simultaneously two tightly

related stochastic processes: the position \mathbf{X}_t and the boundary local time ℓ_t . Once \mathbf{X}_t is constructed, the boundary local time ℓ_t can be obtained by rescaling the residence time of the particle in the thin boundary layer of width a (see [12–25] and references therein):

$$\ell_t = \lim_{a \rightarrow 0} \frac{D}{a} \underbrace{\int_0^t dt' \Theta(a - |\mathbf{X}_{t'} - \partial\Omega|)}_{\text{residence time}}, \quad (2)$$

where $\Theta(z)$ is the Heaviside step function ($\Theta(z) = 1$ for $z > 0$ and 0 otherwise), and $|\mathbf{x} - \partial\Omega|$ denotes the distance between a bulk point \mathbf{x} and the boundary $\partial\Omega$. From equation (2), one can see that the boundary local time ℓ_t is indeed a non-decreasing process that remains constant when \mathbf{X}_t is the bulk, and increases only when \mathbf{X}_t hits the boundary. Even though ℓ_t has units of length, we keep using the canonical term ‘boundary local time’. Note that ℓ_t/D has units of time per length so that its multiplication by the width a of a thin boundary layer approximates the fraction of *time* that the particle spent in that layer up to time t .

Throughout this work, we focus on the common physical setting when the drift represents an external conservative force $\mathbf{F}(\mathbf{x})$, which can be written as the gradient of a potential $V(\mathbf{x})$:

$$\boldsymbol{\mu}(\mathbf{x}) = \frac{\mathbf{F}(\mathbf{x})}{\gamma} = \frac{-\nabla V(\mathbf{x})}{\gamma} = -D\nabla\Phi(\mathbf{x}), \quad (3)$$

where $\Phi(\mathbf{x}) = V(\mathbf{x})/(k_B T)$ is the dimensionless potential and $\gamma = k_B T/D$ is the friction coefficient, with k_B being the Boltzmann’s constant and T the absolute temperature. We emphasize that the drift is time-independent while thermal fluctuations are isotropic and independent of both time and coordinates.

As said earlier, most physical works on restricted diffusion skip the stochastic differential equation (1) and deal directly with the probability density of the position \mathbf{X}_t (also known as the propagator), $G_q(\mathbf{x}, t|\mathbf{x}_0)d\mathbf{x} = \mathbb{P}_{\mathbf{x}_0}\{\mathbf{X}_t \in (\mathbf{x}, \mathbf{x} + d\mathbf{x})\}$, which obeys the Fokker–Planck equation [2]

$$\partial_t G_q(\mathbf{x}, t|\mathbf{x}_0) = \mathcal{L}_x G_q(\mathbf{x}, t|\mathbf{x}_0), \quad (4)$$

where

$$\mathcal{L}_x = -(\nabla_x \cdot \boldsymbol{\mu}(\mathbf{x})) + D\Delta_x \quad (5)$$

is the Fokker–Planck operator. Setting the probability flux density

$$\mathbf{J}_q(\mathbf{x}, t|\mathbf{x}_0) = \boldsymbol{\mu}(\mathbf{x})G_q(\mathbf{x}, t|\mathbf{x}_0) - D\nabla_x G_q(\mathbf{x}, t|\mathbf{x}_0), \quad (6)$$

the Fokker–Planck equation can be understood as the continuity equation expressing the probability conservation: $\partial_t G_q(\mathbf{x}, t|\mathbf{x}_0) = -(\nabla \cdot \mathbf{J}_q)$.

The equation (4) has to be completed by the initial condition $G_q(\mathbf{x}, 0|\mathbf{x}_0) = \delta(\mathbf{x} - \mathbf{x}_0)$ stating that the particle has started from \mathbf{x}_0 at time $t = 0$, and by an appropriate boundary condition that accounts for interactions with the boundary. When the boundary is inert and impermeable for the particle, the probability flux density in the normal direction to the boundary

$$\begin{aligned} j_q(\mathbf{s}, t|\mathbf{x}_0) &= (\mathbf{n}(\mathbf{x}) \cdot \mathbf{J}_q(\mathbf{x}, t|\mathbf{x}_0))|_{\mathbf{x}=\mathbf{s}} \\ &= (\mathbf{n}(\mathbf{s}) \cdot \boldsymbol{\mu}(\mathbf{s}))G_q(\mathbf{s}, t|\mathbf{x}_0) - D(\partial_n G_q(\mathbf{x}, t|\mathbf{x}_0))|_{\mathbf{x}=\mathbf{s}}, \end{aligned} \quad (7)$$

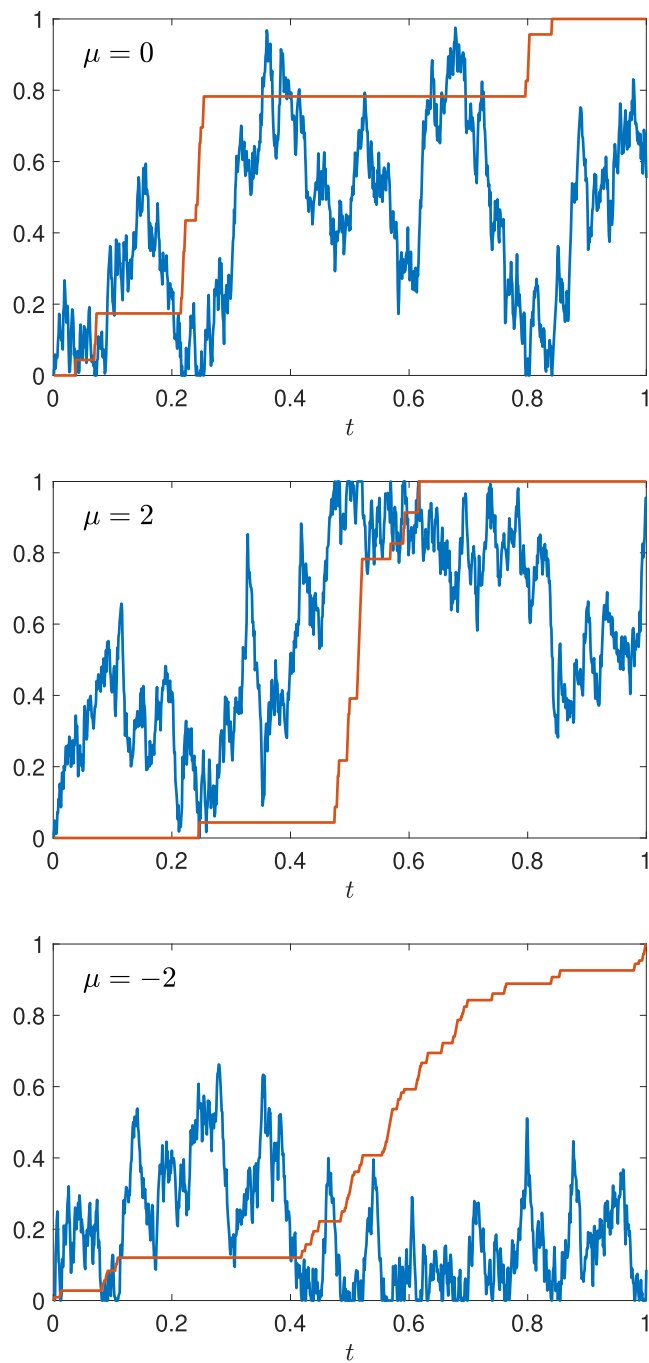


Figure 1. Simulated trajectory X_t (blue line) of restricted diffusion on the unit interval $(0, 1)$ with the starting point $x_0 = 0$ and $D = 1$, and the boundary local time ℓ_t (red line), rescaled by its value ℓ_T at $T = 1$, for three values of the constant drift: $\mu = 0$ (top), $\mu = 2$ (middle) and $\mu = -2$ (bottom). Each trajectory was generated by Monte Carlo simulations with a time step 10^{-3} .

is zero at any boundary point $\mathbf{s} \in \partial\Omega$, with $\partial_n = (\mathbf{n}(\mathbf{x}) \cdot \nabla)$ being the normal derivative oriented outwards the domain Ω . In turn, a partially reactive boundary is often described by *imposing* that the probability flux density in the normal direction is proportional to $G_q(\mathbf{x}, t|\mathbf{x}_0)$,

$$j_q(\mathbf{s}, t|\mathbf{x}_0) = \kappa G_q(\mathbf{s}, t|\mathbf{x}_0) \quad (\mathbf{s} \in \partial\Omega), \tag{8}$$

with κ (in units m s^{-1}) being the reactivity. This Robin-type boundary condition was introduced by Collins and Kimball in the context of chemical physics and was later investigated and employed by many authors [26–41]. When $\kappa = 0$, one retrieves the fully reflecting boundary, whereas in the opposite limit $\kappa \rightarrow \infty$, the left-hand side of this relation vanishes, and one gets the Dirichlet boundary condition $G(\mathbf{x}, t|\mathbf{x}_0)|_{\mathbf{x} \in \partial\Omega} = 0$ for a perfectly reactive boundary. As discussed below, the Robin boundary condition (8) describes one surface reaction mechanism among many others.

It is well known that the propagator also satisfies the backward Fokker–Planck equation [2], which reads in our case as

$$\partial_t G_q(\mathbf{x}, t|\mathbf{x}_0) = \mathcal{L}_{\mathbf{x}_0}^\dagger G_q(\mathbf{x}, t|\mathbf{x}_0), \tag{9}$$

where

$$\mathcal{L}_{\mathbf{x}_0}^\dagger = (\boldsymbol{\mu}(\mathbf{x}_0) \cdot \nabla_{\mathbf{x}_0}) + D\Delta_{\mathbf{x}_0} \tag{10}$$

is the adjoint Fokker–Planck operator. Since both $\boldsymbol{\mu}(\mathbf{x})$ and D are time-independent, solutions of both Fokker–Planck equations depend on the difference between the terminal and starting times t and $t_0 = 0$, that allowed us to replace the time derivative $-\partial_{t_0}$ by ∂_t in equation (9).

The very definition of the propagator $G_q(\mathbf{x}, t|\mathbf{x}_0)$ indicates the deliberate choice of focusing on the position \mathbf{X}_t and ignoring the boundary local time ℓ_t in the second description. As shown in [8] and discussed below, the inclusion of boundary encounters into the theoretical framework brings numerous advantages.

2.2. Full propagator

We start with restricted diffusion without any surface reaction and introduce the full propagator $P(\mathbf{x}, \ell, t|\mathbf{x}_0)$ as the joint probability density of \mathbf{X}_t and ℓ_t in a bounded domain Ω with an *impermeable* boundary $\partial\Omega$:

$$P(\mathbf{x}, \ell, t|\mathbf{x}_0) \mathrm{d}\mathbf{x} \mathrm{d}\ell = \mathbb{P}_{\mathbf{x}_0} \{ \mathbf{X}_t \in (\mathbf{x}, \mathbf{x} + \mathrm{d}\mathbf{x}), \ell_t \in (\ell, \ell + \mathrm{d}\ell) \}. \tag{11}$$

In this way, the full propagator is constructed to describe exclusively the diffusive dynamics in the bulk. As the stochastic solution of the Skorokhod equation (1) is unique [10, 11], the full propagator is well-defined.

In order to incorporate surface reactions, we exploit the microscopic interpretation of the boundary condition (8) by introducing a thin reactive layer of width a near the boundary and counting the number of times, \mathcal{N}_t^a , that the diffusing particle has crossed this layer up to time t . Each crossing can be understood as an encounter with the boundary during which the particle might interact with it. The self-similar character of Brownian motion implies that after the first encounter with the boundary, the particle returns infinitely many times to that boundary [42]. As a consequence, the number \mathcal{N}_t^a diverges as $a \rightarrow 0$, but its rescaling by a yields a nontrivial limit—the boundary local time:

$$\ell_t = \lim_{a \rightarrow 0} a \mathcal{N}_t^a. \tag{12}$$

This representation is equivalent to equation (2) and yields an alternative approximation to the boundary local time.

At each encounter, the particle can react with the boundary with some probability $p_a \simeq a\kappa/D$ or resume its diffusion in the bulk [31, 33, 43]. Such reaction attempts are supposed to be independent from each other and from the diffusion process. Denoting by \mathcal{T} the time of the successful reaction event, one gets in the limit $a \rightarrow 0$:

$$\mathbb{P}\{\mathcal{T} > t\} = \mathbb{E}\{(1 - p_a)^{N_t^a}\} \approx \mathbb{E}\{(1 - a\kappa/D)^{\ell_t/a}\} \approx \mathbb{E}\{e^{-(\kappa/D)\ell_t}\} = \mathbb{P}\{\ell_t < \hat{\ell}\}, \quad (13)$$

where we introduced an independent random threshold $\hat{\ell}$ obeying the exponential law:

$$\mathbb{P}\{\hat{\ell} > \ell\} = e^{-q\ell}, \quad \text{with } q = \kappa/D. \quad (14)$$

In other words, the successful reaction event occurs when the boundary local time ℓ_t crosses the random threshold $\hat{\ell}$. As first suggested in [35], this relation can actually be used as the definition of the first-reaction time \mathcal{T} :

$$\mathcal{T} = \inf\{t > 0 : \ell_t > \hat{\ell}\}, \quad (15)$$

in analogy with the definition of the first-passage time: $\mathcal{T}_{\text{FPT}} = \inf\{t > 0 : X_t \in \partial\Omega\}$. Moreover, as the boundary local time remains zero until the first encounter, the first-passage time can also be defined as $\mathcal{T}_{\text{FPT}} = \inf\{t > 0 : \ell_t > 0\}$, i.e. as the first crossing of the zero threshold. The boundary local time offers thus a unified way of treating perfectly and partially reactive boundaries.

By definition, the conventional propagator $G_q(\mathbf{x}, t|\mathbf{x}_0)$ is the probability density of finding the particle in a vicinity of \mathbf{x} at time t , given that the particle has started at \mathbf{x}_0 and not reacted on the boundary up to time t . According to equation (13), the survival of the particle means that $\ell_t < \hat{\ell}$. As a consequence, the conventional propagator is given by the full propagator $P(\mathbf{x}, \ell, t|\mathbf{x}_0)$, multiplied by the survival probability of that particle up to time t , $\mathbb{P}\{\mathcal{T} > t\} = \mathbb{P}\{\ell_t < \hat{\ell}\}$, and integrated over all possible values of the boundary local time:

$$G_q(\mathbf{x}, t|\mathbf{x}_0) = \int_0^\infty d\ell \underbrace{e^{-q\ell}}_{=\mathbb{P}\{\ell < \hat{\ell}\}} P(\mathbf{x}, \ell, t|\mathbf{x}_0). \quad (16)$$

The parameter q stands in the subscript of the propagator to highlight its dependence on q through the boundary condition (8). In other words, the propagator for partially reactive boundary is obtained as the Laplace transform (with respect to ℓ) of the full propagator for purely reflecting boundary. This relation was established in [8] for ordinary diffusion without drift. Whenever surface reactions are independent from bulk dynamics, the above arguments can be applied, in particular, equation (16) holds for more general diffusion processes with a drift. Note also that this relation can also be deduced from the rigorous probabilistic analysis of a more general Robin boundary value problem presented in [44]. We emphasize that the boundary local time ℓ_t depends exclusively on the diffusive dynamics in the confining domain Ω with a purely reflecting boundary, whereas the threshold $\hat{\ell}$ depends exclusively on the reactivity q , allowing one to disentangle these two aspects of diffusion-controlled reactions. This disentanglement opens a way to investigate much more elaborate surface reaction mechanisms when the exponential distribution of the random threshold $\hat{\ell}$ is replaced by another distribution (see [8] for details). As a consequence, the unique full propagator $P(\mathbf{x}, \ell, t|\mathbf{x}_0)$ can determine a variety of conventional propagators by choosing an appropriate stopping condition. In summary, the stochastic foundation (1) for both conventional and encounter-based approaches is the same,

but the ways of incorporating surface reactions are different (Robin boundary condition versus random threshold $\hat{\ell}$).

While the full propagator $P(\mathbf{x}, \ell, t|\mathbf{x}_0)$ determines any conventional propagator $G_q(\mathbf{x}, t|\mathbf{x}_0)$ via equation (16), its inverse Laplace transform with respect to q can in turn be used to access the full propagator. However, the implicit dependence of the conventional propagator on q as the parameter in the boundary condition (8) makes difficult further explorations of such an inverse, even numerically. To overcome this limitation, a spectral representation of the full propagator was derived in [8] for ordinary diffusion. Here we aim at extending this representation to restricted diffusion with a gradient drift.

2.3. Spectral decompositions

In the following, we mainly deal with Laplace-transformed quantities with respect to time t , denoted by tilde. For instance,

$$\tilde{G}_q(\mathbf{x}, p|\mathbf{x}_0) = \int_0^\infty dt e^{-pt} G_q(\mathbf{x}, t|\mathbf{x}_0) \tag{17}$$

is the Green's function for the Fokker-Planck equation, which admits both forward and backward forms:

$$\begin{cases} (p - \mathcal{L}_x)\tilde{G}_q(\mathbf{x}, p|\mathbf{x}_0) = \delta(\mathbf{x} - \mathbf{x}_0) & (\mathbf{x} \in \Omega) \\ \tilde{j}_q(\mathbf{x}, p|\mathbf{x}_0) = \kappa\tilde{G}_q(\mathbf{x}, p|\mathbf{x}_0) & (\mathbf{x} \in \partial\Omega) \end{cases} \quad \text{(forward)} \tag{18}$$

and

$$\begin{cases} (p - \mathcal{L}_{x_0}^\dagger)\tilde{G}_q(\mathbf{x}, p|\mathbf{x}_0) = \delta(\mathbf{x} - \mathbf{x}_0) & (\mathbf{x}_0 \in \Omega) \\ \partial_{n_0}\tilde{G}_q(\mathbf{x}, p|\mathbf{x}_0) + q\tilde{G}_q(\mathbf{x}, p|\mathbf{x}_0) = 0 & (\mathbf{x}_0 \in \partial\Omega) \end{cases} \quad \text{(backward)}, \tag{19}$$

where

$$\tilde{j}_q(\mathbf{x}, p|\mathbf{x}_0) = (\mathbf{n}(\mathbf{x}) \cdot \boldsymbol{\mu}(\mathbf{x}))\tilde{G}_q(\mathbf{x}, p|\mathbf{x}_0) - D\partial_n\tilde{G}_q(\mathbf{x}, p|\mathbf{x}_0) \quad (\mathbf{x} \in \partial\Omega) \tag{20}$$

is the Laplace-transformed probability flux density.

In [8], we considered ordinary restricted diffusion (without drift) and employed the so-called Dirichlet-to-Neumann operator \mathcal{M}_p that associates to a given function f on the boundary $\partial\Omega$ another function on that boundary such that $\mathcal{M}_p f = (\partial_n u)|_{\partial\Omega}$, where $u(\mathbf{x})$ satisfies $(p - D\Delta)u(\mathbf{x}) = 0$ in Ω and $u|_{\partial\Omega} = f$. In other words, \mathcal{M}_p maps the Dirichlet boundary condition onto Neumann boundary condition. Relying on the fact that the self-adjoint operator \mathcal{M}_p on a bounded boundary has a discrete spectrum (see [45–51] for mathematical details), we derived the following spectral decomposition

$$\tilde{G}_q(\mathbf{x}, p|\mathbf{x}_0) = \tilde{G}_\infty(\mathbf{x}, p|\mathbf{x}_0) + \frac{1}{D} \sum_n \frac{V_n^{(p)}(\mathbf{x})[V_n^{(p)}(\mathbf{x}_0)]^*}{q + \mu_n^{(p)}}, \tag{21}$$

where $\mu_n^{(p)}$ are the eigenvalues of \mathcal{M}_p , while $V_n^{(p)}(\mathbf{x})$ are projections of $\tilde{j}_\infty(\mathbf{x}, p|\mathbf{x}_0)$ onto the eigenfunctions $v_n^{(p)}$ of that operator (see below for details; note that equation (21) is not used in the following derivation and is reproduced here just for motivation). The inverse Laplace transform of this relation with respect to q yielded the spectral decomposition of the Laplace-transformed full propagator:

$$\tilde{P}_q(\mathbf{x}, \ell, p|\mathbf{x}_0) = \tilde{G}_\infty(\mathbf{x}, p|\mathbf{x}_0)\delta(\ell) + \frac{1}{D} \sum_n V_n^{(p)}(\mathbf{x}) [V_n^{(p)}(\mathbf{x}_0)]^* e^{-\ell\mu_n^{(p)}}. \quad (22)$$

A naive extension of this approach to restricted diffusion with drift would fail. In fact, even though an appropriate Dirichlet-to-Neumann operator could be introduced by replacing the equation $(p - D\Delta)u = 0$ by $(p - \mathcal{L}_x)u = 0$ or $(p - \mathcal{L}_{x_0}^\dagger)u = 0$, such an extension would not in general be self-adjoint and thus would require much more elaborate spectral tools.

To overcome this limitation, we reformulate the problem in terms of the symmetrized Fokker–Planck operator [2]

$$\bar{\mathcal{L}} = De^{\frac{1}{2}\Phi(\mathbf{x})}\nabla_x e^{-\Phi(\mathbf{x})}\nabla_x e^{\frac{1}{2}\Phi(\mathbf{x})} = D\Delta - \left(\frac{(\nabla \cdot \boldsymbol{\mu}(\mathbf{x}))}{2} + \frac{|\boldsymbol{\mu}(\mathbf{x})|^2}{4D} \right), \quad (23)$$

where the second term in the last relation is the multiplication by the explicit drift-dependent function (here, the operator ∇ acts only on $\boldsymbol{\mu}(\mathbf{x})$). To avoid mathematical subtleties, we assume that the second term is a smooth bounded function on Ω . With the aid of this expression, the Fokker–Planck operator and its adjoint can be written as

$$\mathcal{L} = e^{-\frac{1}{2}\Phi(\mathbf{x})}\bar{\mathcal{L}}e^{\frac{1}{2}\Phi(\mathbf{x})} = D\nabla_x e^{-\Phi(\mathbf{x})}\nabla_x e^{\Phi(\mathbf{x})}, \quad (24)$$

$$\mathcal{L}^\dagger = e^{\frac{1}{2}\Phi(\mathbf{x})}\bar{\mathcal{L}}e^{-\frac{1}{2}\Phi(\mathbf{x})} = De^{\Phi(\mathbf{x})}\nabla_x e^{-\Phi(\mathbf{x})}\nabla_x. \quad (25)$$

In order to reduce the original problem to that with $\bar{\mathcal{L}}$, one can represent the Green’s function as

$$\tilde{G}_q(\mathbf{x}, p|\mathbf{x}_0) = e^{\frac{1}{2}\Phi(\mathbf{x}_0) - \frac{1}{2}\Phi(\mathbf{x})}\tilde{g}_q(\mathbf{x}, p|\mathbf{x}_0), \quad (26)$$

so that forward and backward equations imply two equivalent boundary value problems for the new function $\tilde{g}_q(\mathbf{x}, p|\mathbf{x}_0)$:

$$(p - \bar{\mathcal{L}}_x)\tilde{g}_q(\mathbf{x}, p|\mathbf{x}_0) = \delta(\mathbf{x} - \mathbf{x}_0) \quad (\mathbf{x} \in \Omega), \quad (27)$$

$$(\partial_n + q + \phi(\mathbf{x}))\tilde{g}_q(\mathbf{x}, p|\mathbf{x}_0) = 0 \quad (\mathbf{x} \in \partial\Omega), \quad (28)$$

and

$$(p - \bar{\mathcal{L}}_{x_0})\tilde{g}_q(\mathbf{x}, p|\mathbf{x}_0) = \delta(\mathbf{x} - \mathbf{x}_0) \quad (\mathbf{x}_0 \in \Omega), \quad (29)$$

$$(\partial_{n_0} + q + \phi(\mathbf{x}_0))\tilde{g}_q(\mathbf{x}, p|\mathbf{x}_0) = 0 \quad (\mathbf{x}_0 \in \partial\Omega), \quad (30)$$

with

$$\phi(\mathbf{x}) = \frac{1}{2}(\partial_n \Phi(\mathbf{x})) = -\frac{1}{2D}(\mathbf{n}(\mathbf{x}) \cdot \boldsymbol{\mu}(\mathbf{x})) \quad (\mathbf{x} \in \partial\Omega). \quad (31)$$

As the forward and backward problems are now identical, their solution is symmetric with respect to the exchange of \mathbf{x} and \mathbf{x}_0 : $\tilde{g}_q(\mathbf{x}, p|\mathbf{x}_0) = \tilde{g}_q(\mathbf{x}_0, p|\mathbf{x})$.

We search for the following representation:

$$\tilde{g}_q(\mathbf{x}, p|\mathbf{x}_0) = \tilde{g}_\infty(\mathbf{x}, p|\mathbf{x}_0) + \frac{1}{D}u(\mathbf{x}, p|\mathbf{x}_0), \quad (32)$$

where the new function $u(\mathbf{x}, p|\mathbf{x}_0)$ satisfies

$$(p - \bar{\mathcal{L}}_{\mathbf{x}_0})u(\mathbf{x}, p|\mathbf{x}_0) = 0, \tag{33}$$

subject to the boundary condition at $\mathbf{x}_0 \in \partial\Omega$:

$$\begin{aligned} 0 &= (\partial_{n_0} + q)\tilde{G}_q(\mathbf{x}, p|\mathbf{x}_0) \\ &= (\partial_{n_0} + q) \left(\tilde{G}_\infty(\mathbf{x}, p|\mathbf{x}_0) + \frac{e^{\frac{1}{2}\Phi(\mathbf{x}_0) - \frac{1}{2}\Phi(\mathbf{x})}}{D} u(\mathbf{x}, p|\mathbf{x}_0) \right) \\ &= \partial_{n_0}\tilde{G}_\infty(\mathbf{x}, p|\mathbf{x}_0) + \frac{e^{\frac{1}{2}\Phi(\mathbf{x}_0) - \frac{1}{2}\Phi(\mathbf{x})}}{D} (\partial_{n_0} + q + \phi(\mathbf{x}_0)) u(\mathbf{x}, p|\mathbf{x}_0), \end{aligned}$$

i.e.

$$(\partial_{n_0} + q + \phi(\mathbf{x}_0)) u(\mathbf{x}, p|\mathbf{x}_0) = e^{\frac{1}{2}\Phi(\mathbf{x}) - \frac{1}{2}\Phi(\mathbf{x}_0)} \tilde{j}'_\infty(\mathbf{x}_0, p|\mathbf{x}) \quad (\mathbf{x}_0 \in \partial\Omega), \tag{34}$$

where

$$\tilde{j}'_\infty(\mathbf{x}_0, p|\mathbf{x}) = -D\partial_{n_0}\tilde{G}_\infty(\mathbf{x}, p|\mathbf{x}_0) \quad (\mathbf{x}_0 \in \partial\Omega). \tag{35}$$

Since the normal derivative ∂_{n_0} acts on \mathbf{x}_0 of $\tilde{G}_q(\mathbf{x}, p|\mathbf{x}_0)$, this function differs in general from $\tilde{j}'_\infty(\mathbf{x}, p|\mathbf{x}_0)$ given in equation (20). We also emphasize that the order of \mathbf{x}_0 and \mathbf{x} in this notation has been changed, in order to keep the convention that the first argument of j is a point on the boundary.

In the next step, we introduce a Dirichlet-to-Neumann operator \mathcal{M}_p that associates to a given function f on $\partial\Omega$ another function on $\partial\Omega$ such that

$$\mathcal{M}_p f = (\partial_n w + \phi(\mathbf{x})w)|_{\partial\Omega}, \quad \text{with} \quad \begin{cases} (p - \bar{\mathcal{L}}_{\mathbf{x}})w = 0 & (\mathbf{x} \in \Omega), \\ w = f & (\mathbf{x} \in \partial\Omega). \end{cases} \tag{36}$$

The operator $\bar{\mathcal{L}}$ in equation (23) having the form of a Schrödinger operator, is self-adjoint; in addition, as the domain is bounded, the drift-dependent term is a bounded perturbation to the Laplace operator. In analogy with the Laplacian case (see [47, 48] for mathematical details), one can expect that, under mild assumptions on the drift term, the Dirichlet-to-Neumann operator \mathcal{M}_p is self-adjoint, with a discrete spectrum of real eigenvalues $\{\mu_n^{(p)}\}$, while its eigenfunctions $\{v_n^{(p)}\}$ form a complete orthonormal basis in $L_2(\partial\Omega)$. As a proof of this mathematical statement is beyond the scope of the present paper, we will use it as a conjecture in the following presentation. In other words, we focus on such drifts $\boldsymbol{\mu}(\mathbf{x})$, for which this statement is valid. The Dirichlet-to-Neumann operator \mathcal{M}_p allows us to rewrite the boundary condition (34) in an operator form, from which

$$u(\mathbf{x}, p|\mathbf{x}_0) = (\mathcal{M}_p + q)^{-1} e^{\frac{1}{2}\Phi(\mathbf{x}) - \frac{1}{2}\Phi(\mathbf{x}_0)} \tilde{j}'_\infty(\mathbf{x}_0, p|\mathbf{x}) \quad (\mathbf{x}_0 \in \partial\Omega). \tag{37}$$

Finally, one needs to extend $u(\mathbf{x}, p|\mathbf{x}_0)$ to any $\mathbf{x}_0 \in \Omega$. For this purpose, one multiplies equation (27) with $q = \infty$ by $u(\mathbf{x}, p|\mathbf{x}')$ and subtracts from it the equation $(p - \bar{\mathcal{L}}_{\mathbf{x}})u(\mathbf{x}, p|\mathbf{x}') = 0$ multiplied by $\tilde{g}_\infty(\mathbf{x}', p|\mathbf{x}_0)$. The integration of both parts over \mathbf{x}' yields

$$\begin{aligned}
 u(\mathbf{x}, p|\mathbf{x}_0) &= \int_{\Omega} d\mathbf{x}' u(\mathbf{x}, p|\mathbf{x}') \delta(\mathbf{x}' - \mathbf{x}_0) \\
 &= \int_{\Omega} d\mathbf{x}' (u(\mathbf{x}, p|\mathbf{x}') (p - \bar{\mathcal{L}}_{\mathbf{x}'} \tilde{g}_{\infty}(\mathbf{x}', p|\mathbf{x}_0) - \tilde{g}_{\infty}(\mathbf{x}', p|\mathbf{x}_0) (p - \bar{\mathcal{L}}_{\mathbf{x}'} u(\mathbf{x}, p|\mathbf{x}')) \\
 &= - \int_{\Omega} d\mathbf{x}' (u(\mathbf{x}, p|\mathbf{x}') D \Delta_{\mathbf{x}'} \tilde{g}_{\infty}(\mathbf{x}', p|\mathbf{x}_0) - \tilde{g}_{\infty}(\mathbf{x}', p|\mathbf{x}_0) D \Delta_{\mathbf{x}'} u(\mathbf{x}, p|\mathbf{x}')) \\
 &= - \int_{\partial\Omega} d\mathbf{x}' (u(\mathbf{x}, p|\mathbf{x}') D \partial_{n'} \tilde{g}_{\infty}(\mathbf{x}', p|\mathbf{x}_0) - \tilde{g}_{\infty}(\mathbf{x}', p|\mathbf{x}_0) D \partial_{n'} u(\mathbf{x}, p|\mathbf{x}')) \\
 &= \int_{\partial\Omega} d\mathbf{x}' u(\mathbf{x}, p|\mathbf{x}') e^{\frac{1}{2}\Phi(\mathbf{x}') - \frac{1}{2}\Phi(\mathbf{x}_0)} \partial_{n'} (-D \tilde{G}_{\infty}(\mathbf{x}', p|\mathbf{x}_0)) \\
 &= \int_{\partial\Omega} d\mathbf{x}' u(\mathbf{x}, p|\mathbf{x}') e^{\frac{1}{2}\Phi(\mathbf{x}') - \frac{1}{2}\Phi(\mathbf{x}_0)} \tilde{j}_{\infty}(\mathbf{x}', p|\mathbf{x}_0),
 \end{aligned}$$

where we used Green's relations and the Dirichlet boundary condition $\tilde{G}_{\infty}(\mathbf{x}, p|\mathbf{x}_0) = 0$ at $\mathbf{x} \in \partial\Omega$. As a consequence, we get

$$\begin{aligned}
 \tilde{G}_q(\mathbf{x}, p|\mathbf{x}_0) &= \tilde{G}_{\infty}(\mathbf{x}, p|\mathbf{x}_0) + \frac{e^{\frac{1}{2}\Phi(\mathbf{x}_0) - \frac{1}{2}\Phi(\mathbf{x})}}{D} u(\mathbf{x}, p|\mathbf{x}_0) \\
 &= \tilde{G}_{\infty}(\mathbf{x}, p|\mathbf{x}_0) + \frac{e^{-\frac{1}{2}\Phi(\mathbf{x})}}{D} \int_{\partial\Omega} d\mathbf{x}' u(\mathbf{x}, p|\mathbf{x}') e^{\frac{1}{2}\Phi(\mathbf{x}')} \tilde{j}_{\infty}(\mathbf{x}', p|\mathbf{x}_0) \\
 &= \tilde{G}_{\infty}(\mathbf{x}, p|\mathbf{x}_0) + \frac{1}{D} \int_{\partial\Omega} d\mathbf{x}' \left((\mathcal{M}_p + q)^{-1} e^{-\frac{1}{2}\Phi(\mathbf{x}')} \tilde{j}_{\infty}(\mathbf{x}', p|\mathbf{x}) \right) \\
 &\quad \times e^{\frac{1}{2}\Phi(\mathbf{x}')} \tilde{j}_{\infty}(\mathbf{x}', p|\mathbf{x}_0). \tag{38}
 \end{aligned}$$

Using the eigenfunctions of \mathcal{M}_p , one gets the spectral decomposition of the Green's function:

$$\tilde{G}_q(\mathbf{x}, p|\mathbf{x}_0) = \tilde{G}_{\infty}(\mathbf{x}, p|\mathbf{x}_0) + \frac{1}{D} \sum_n \frac{V_n^{(p)}(\mathbf{x}) [V_n^{(p)}(\mathbf{x}_0)]^*}{q + \mu_n^{(p)}}, \tag{39}$$

where

$$V_n^{(p)}(\mathbf{x}_0) = \int_{\partial\Omega} d\mathbf{s} v_n^{(p)}(\mathbf{s}) e^{\frac{1}{2}\Phi(\mathbf{s})} \tilde{j}_{\infty}(\mathbf{s}, p|\mathbf{x}_0), \tag{40}$$

$$V_n^{(p)}(\mathbf{x}) = \int_{\partial\Omega} d\mathbf{s} v_n^{(p)}(\mathbf{s}) e^{-\frac{1}{2}\Phi(\mathbf{s})} \tilde{j}_{\infty}(\mathbf{s}, p|\mathbf{x}). \tag{41}$$

When there is no drift, one has $\Phi(\mathbf{s}) = 0$ and thus $V_n^{(p)}(\mathbf{x}) = V_n^{(p)}(\mathbf{x})$, so that equation (39) is reduced to the former result (21) derived in [8]. The Laplace inversion of equation (39) with

respect to q yields

$$\tilde{P}(\mathbf{x}, \ell, p|\mathbf{x}_0) = \tilde{G}_\infty(\mathbf{x}, p|\mathbf{x}_0)\delta(\ell) + \frac{1}{D} \sum_n V_n^{(p)}(\mathbf{x}) [V_n^{(p)}(\mathbf{x}_0)]^* e^{-\ell\mu_n^{(p)}}. \quad (42)$$

This is our main theoretical result, which generalizes the former relation (22) to the case of restricted diffusion with a gradient drift.

2.4. Various diffusion–reaction characteristics

As said earlier, the full propagator determines various characteristics of diffusion-influenced reactions. For instance, integrating equations (39) and (42) over $\mathbf{x} \in \Omega$, one accesses the Laplace-transformed survival probability and the Laplace-transformed probability density of the boundary local time, respectively:

$$\tilde{S}_q(p|\mathbf{x}_0) = \tilde{S}_\infty(p|\mathbf{x}_0) + \frac{1}{D} \sum_n \frac{\overline{V_n^{(p)}} [V_n^{(p)}(\mathbf{x}_0)]^*}{q + \mu_n^{(p)}}, \quad (43)$$

and

$$\tilde{P}(\circ, \ell, p|\mathbf{x}_0) = \tilde{S}_\infty(p|\mathbf{x}_0)\delta(\ell) + \frac{1}{D} \sum_n \overline{V_n^{(p)}} [V_n^{(p)}(\mathbf{x}_0)]^* e^{-\ell\mu_n^{(p)}}, \quad (44)$$

where \circ denotes the marginalized variable \mathbf{x} , and

$$\overline{V_n^{(p)}} = \int_\Omega d\mathbf{x} V_n^{(p)}(\mathbf{x}). \quad (45)$$

In appendix A, we derive the following representation for this quantity:

$$\overline{V_n^{(p)}} = \frac{D}{p} \mu_n^{(p)} \int_{\partial\Omega} ds e^{-\frac{1}{2}\Phi(s)} v_n^{(p)}(s). \quad (46)$$

These expressions generalize our former results for ordinary diffusion without drift from [52, 53].

We recall that the survival probability determines the distribution of the first-reaction time \mathcal{T} on a partially reactive boundary [4]: $S_q(t|\mathbf{x}_0) = \mathbb{P}_{\mathbf{x}_0}\{\mathcal{T} > t\}$. At the same time, $S_q(t|\mathbf{x}_0) = \mathbb{E}_{\mathbf{x}_0}\{e^{-q\ell_t}\}$ is the generating function of the boundary local time ℓ_t [8, 41] that allows one to compute its moments as

$$\mathbb{E}_{\mathbf{x}_0}\{\ell_t^k\} = (-1)^k \lim_{q \rightarrow 0} \frac{\partial^k}{\partial q^k} S_q(t|\mathbf{x}_0), \quad (47)$$

from which

$$\int_0^\infty dt e^{-pt} \mathbb{E}_{\mathbf{x}_0}\{\ell_t^k\} = \frac{k!}{D} \sum_n \frac{\overline{V_n^{(p)}} [V_n^{(p)}(\mathbf{x}_0)]^*}{[\mu_n^{(p)}]^{k+1}}. \quad (48)$$

Multiplying both sides by p , one can also interpret the integral over t as the double average of the random variable ℓ_τ^k with the random exponentially distributed stopping time τ . Similarly,

$p\tilde{P}(\circ, \ell, p|\mathbf{x}_0)$ can be interpreted as the probability density of ℓ_τ :

$$\mathbb{P}_{\mathbf{x}_0}\{\ell_\tau \in (\ell, \ell + d\ell)\} = \int_0^\infty dt \underbrace{p e^{-pt}}_{\text{pdf of } \tau} \mathbb{P}_{\mathbf{x}_0}\{\ell_t \in (\ell, \ell + d\ell)\} = p\tilde{P}(\circ, \ell, p|\mathbf{x}_0)d\ell. \quad (49)$$

Setting $q = 0$ in equation (43) and noting that $\tilde{S}_0(p|\mathbf{x}_0) = 1/p$ (since $S_0(t|\mathbf{x}_0) = 1$ for a fully inert boundary), one gets

$$\tilde{S}_\infty(p|\mathbf{x}_0) = \frac{1}{p} - \frac{1}{D} \sum_n \frac{\overline{V_n^{(p)}} [V_n^{(p)}(\mathbf{x}_0)]^*}{\mu_n^{(p)}}. \quad (50)$$

Substituting this expression back into equation (43), one deduces an equivalent spectral decomposition:

$$\tilde{S}_q(p|\mathbf{x}_0) = \frac{1}{p} - \frac{1}{D} \sum_n \frac{\overline{V_n^{(p)}} [V_n^{(p)}(\mathbf{x}_0)]^*}{\mu_n^{(p)}(1 + \mu_n^{(p)}/q)}, \quad (51)$$

from which one also derives the Laplace-transformed probability density of the first-reaction time:

$$\tilde{H}_q(p|\mathbf{x}_0) = 1 - p\tilde{S}_q(p|\mathbf{x}_0) = \frac{p}{D} \sum_n \frac{\overline{V_n^{(p)}} [V_n^{(p)}(\mathbf{x}_0)]^*}{\mu_n^{(p)}(1 + \mu_n^{(p)}/q)}. \quad (52)$$

As $H_q(t|\mathbf{x}_0)$ can be interpreted as the probability flux of particles, started from \mathbf{x}_0 , onto the reactive boundary, the total flux $J_q(t)$ is obtained by averaging $H_q(t|\mathbf{x}_0)$ with the initial concentration $c(\mathbf{x}_0)$ of these particles. If the initial concentration is uniform, $c(\mathbf{x}_0) = c_0$, one gets in the Laplace domain:

$$\tilde{J}_q(p) = \int_\Omega d\mathbf{x}_0 c_0 \tilde{H}_q(p|\mathbf{x}_0) = c_0 \frac{p}{D} \sum_n \frac{\overline{V_n^{(p)}} [V_n^{(p)}]^*}{\mu_n^{(p)}(1 + \mu_n^{(p)}/q)}, \quad (53)$$

where

$$\overline{V_n^{(p)}} = \int_\Omega d\mathbf{x}_0 V_n^{(p)}(\mathbf{x}_0). \quad (54)$$

Finally, the definition (15) of the first-reaction time \mathcal{T} puts forward the importance of threshold crossing by the boundary local time ℓ_t . Following [8], let us consider a fixed threshold ℓ and investigate its first-crossing time $\mathcal{T}_\ell = \inf\{t > 0 : \ell_t > \ell\}$ (note that $\mathcal{T} = \mathcal{T}_{\hat{\ell}}$, i.e. when a fixed threshold ℓ is replaced by a random threshold $\hat{\ell}$). As the boundary local time is a non-decreasing process, one has $\mathbb{P}\{\mathcal{T}_\ell > t\} = \mathbb{P}\{\ell_t < \ell\}$, from which the probability density $U(\ell, t|\mathbf{x}_0)$ of \mathcal{T}_ℓ can be expressed as

$$U(\ell, t|\mathbf{x}_0) = -\partial_t \mathbb{P}\{\mathcal{T}_\ell > t\} = \partial_t \mathbb{P}\{\ell_t > \ell\} = \partial_t \int_\ell^\infty d\ell' P(\circ, \ell', t|\mathbf{x}_0). \quad (55)$$

In the Laplace domain, the substitution of equation (44) yields

$$\tilde{U}(\ell, p|\mathbf{x}_0) = \frac{p}{D} \sum_n \frac{\overline{V_n^{(p)}} [V_n^{(p)}(\mathbf{x}_0)]^*}{\mu_n^{(p)}} e^{-\ell \mu_n^{(p)}}. \quad (56)$$

As $\mathcal{T} = \mathcal{T}_{\hat{\ell}}$, the probability densities of \mathcal{T} and $\mathcal{T}_{\hat{\ell}}$ are related:

$$\begin{aligned} H_q(t|\mathbf{x}_0) &= \frac{d\mathbb{P}\{\mathcal{T} \in (t, t + dt)\}}{dt} = \int_0^\infty d\ell qe^{-q\ell} \frac{d\mathbb{P}\{\mathcal{T}_{\hat{\ell}} \in (t, t + dt)\}}{dt} \\ &= \int_0^\infty d\ell qe^{-q\ell} U(\ell, t|\mathbf{x}_0), \end{aligned}$$

where $qe^{-q\ell}$ is the probability density of the exponential threshold $\hat{\ell}$. As the full propagator determines a variety of conventional propagators, the probability density $U(\ell, t|\mathbf{x}_0)$ determines a variety of the first-reaction time densities.

2.5. Probabilistic interpretation

To conclude this section, we provide some probabilistic insights onto the above results. For this purpose, we write an alternative representation of the Green's function:

$$\begin{aligned} \tilde{G}_q(\mathbf{x}, p|\mathbf{x}_0) &= \tilde{G}_\infty(\mathbf{x}, p|\mathbf{x}_0) + \int_{\partial\Omega} ds_1 \int_{\partial\Omega} ds_2 \tilde{j}_\infty(s_1, p|\mathbf{x}_0) \tilde{G}_q \\ &\quad \times (s_2, p|s_1) \tilde{j}'_\infty(s_2, p|\mathbf{x}). \end{aligned} \tag{57}$$

This relation claims that either a random trajectory starting from \mathbf{x}_0 goes directly to \mathbf{x} without hitting the boundary (the first term), or this trajectory hits the boundary at least once before arriving at \mathbf{x} (the second term). In the latter case, the Markov property of restricted diffusion implies the product of three contributions in the Laplace domain: the particle hits the boundary for the first time at some point s_1 (the factor $\tilde{j}_\infty(s_1, p|\mathbf{x}_0)$), moves inside the domain until the last hit of the boundary at some point s_2 (the factor $\tilde{G}_q(s_2, p|s_1)$), and finally goes directly to the bulk point \mathbf{x} (the factor $\tilde{j}'_\infty(s_2, p|\mathbf{x})$). A direct definition of the last factor would require conditioning Brownian trajectories to avoid hitting the boundary. A simpler approach consists in the simultaneous time and drift reversal (i.e. $\boldsymbol{\mu}(\mathbf{x}) \rightarrow -\boldsymbol{\mu}(\mathbf{x})$) in the diffusive dynamics, for which $\tilde{j}'_\infty(s_2, t|\mathbf{x})$ can be understood as the probability flux density onto the absorbing boundary at the point s_2 at time t when starting from \mathbf{x} . In this way, one restores the reversal symmetry of restricted diffusion, in particular, one gets $G'_q(\mathbf{x}_0, t|\mathbf{x}) = G_q(\mathbf{x}, t|\mathbf{x}_0)$ and thus

$$\tilde{j}'_\infty(\mathbf{x}_0, p|\mathbf{x}) = -D\partial_{n_0} \tilde{G}'_\infty(\mathbf{x}_0, p|\mathbf{x}). \tag{58}$$

When there is no drift, one simply has $G_q(\mathbf{x}_0, t|\mathbf{x}) = G'_q(\mathbf{x}_0, t|\mathbf{x}) = G_q(\mathbf{x}, t|\mathbf{x}_0)$ and also $\tilde{j}'_\infty(s, t|\mathbf{x}) = j_\infty(s, t|\mathbf{x})$.

Comparison of equations (38) and (57) implies that

$$(\mathcal{M}_p + q)_{s_1} \underbrace{De^{\frac{1}{2}\Phi(s_2) - \frac{1}{2}\Phi(s_1)} \tilde{G}_q(s_2, p|s_1)}_{=\tilde{g}_q(s_2, p|s_1)} = \delta(s_1 - s_2) \quad (s_1, s_2 \in \partial\Omega),$$

i.e. $D\tilde{g}_q(s_2, p|s_1)$ can be understood as the kernel density of the operator $(\mathcal{M}_p + q)^{-1}$.

3. Constant drift on an interval

In order to illustrate the derived spectral decompositions, we consider a simple yet informative setting of restricted diffusion on an interval $(0, L)$ with a constant drift μ . This problem is mathematically equivalent to restricted diffusion between parallel plates given that the lateral

motion along the plates does not affect boundary encounters. For instance, this mathematical setting can describe the motion of a charged particle in a constant electric field inside a capacitor. The geometric simplicity of the problem will allow us to get fully explicit formulas and thus to clearly illustrate the effect of the drift onto the statistics of boundary encounters. Qualitatively, a drift toward the boundary tends to keep the particle in a vicinity of the boundary and thus to enlarge the number of encounters, whereas the reversed drift is expected to result in the opposite effect. However, these effects have not been studied quantitatively, to our knowledge.

The constant drift corresponds to the potential $\Phi(x) = -\mu x/D$. Expectedly, the Fokker–Planck operator $\mathcal{L} = D\partial_x^2 - \mu\partial_x$ is not self-adjoint, whereas the symmetric operator, which takes a simple form

$$\bar{\mathcal{L}} = D\partial_x^2 - \mu^2/(4D) = D(\partial_x^2 - \gamma^2), \quad \gamma = -\frac{\mu}{2D}, \tag{59}$$

is self-adjoint.

3.1. Dirichlet-to-Neumann operator

As the boundary of an interval consists of two endpoints, the pseudo-differential operator \mathcal{M}_p is reduced to a 2×2 matrix. In fact, a general solution of the equation $(p - \bar{\mathcal{L}})u = 0$ has the form $u(x) = c_+e^{\beta x} + c_-e^{-\beta x}$, with $\beta = \sqrt{p/D + \gamma^2}$ and two coefficients c_{\pm} to be fixed by boundary conditions. Any ‘function’ on the boundary can thus be obtained as a superposition of two linearly independent vectors: $f_1 = (1, 0)^\dagger$ and $f_2 = (0, 1)^\dagger$, where the first and second components stand for the values at the endpoints $x = 0$ and $x = L$, respectively. According to equation (36), the operator \mathcal{M}_p acts as

$$\mathcal{M}_p \begin{pmatrix} u(0) \\ u(L) \end{pmatrix} = \begin{pmatrix} (\partial_n u)_{x=0} + \phi(0)u(0) \\ (\partial_n u)_{x=L} + \phi(L)u(L) \end{pmatrix}, \tag{60}$$

where $\phi(0) = -\frac{1}{2}(\partial_x \Phi)_{x=0} = \mu/(2D) = -\gamma$ and $\phi(L) = \frac{1}{2}(\partial_x \Phi)_{x=L} = \gamma$. The boundary ‘function’ $f_1 = (1, 0)^\dagger$ is obtained with

$$c_+ = \frac{-1}{e^{2\beta L} - 1}, \quad c_- = \frac{1}{1 - e^{-2\beta L}}, \tag{61}$$

while $f_2 = (0, 1)^\dagger$ corresponds to

$$c_+ = \frac{e^{\beta L}}{e^{2\beta L} - 1}, \quad c_- = -\frac{e^{\beta L}}{e^{2\beta L} - 1}. \tag{62}$$

We get then

$$\mathcal{M}_p = \begin{pmatrix} \beta \operatorname{ctanh}(\beta L) - \gamma & -\beta / \sinh(\beta L) \\ -\beta / \sinh(\beta L) & \beta \operatorname{ctanh}(\beta L) + \gamma \end{pmatrix}. \tag{63}$$

Expectedly, this is a Hermitian matrix with two real positive eigenvalues,

$$\mu_{\pm}^{(p)} = \beta \operatorname{ctanh}(\beta L) \pm \sqrt{\gamma^2 + \frac{\beta^2}{\sinh^2(\beta L)}}, \tag{64}$$

and orthonormal eigenvectors:

$$v_{\pm}^{(p)} = \frac{-1}{\sqrt{(\mu_{\pm}^{(p)} - (\mathcal{M}_p)_{11})^2 + (\mathcal{M}_p)_{12}^2}} \begin{pmatrix} (\mathcal{M}_p)_{12} \\ \mu_{\pm}^{(p)} - (\mathcal{M}_p)_{11} \end{pmatrix}. \quad (65)$$

To distinguish two eigenmodes, here we use the subscripts + and – instead of the index n employed in section 2.

3.2. Dirichlet Green’s function

To complete the computation, one needs to evaluate the probability flux densities. In appendix B, we recall the derivation of the Green’s function on the interval. For perfectly reactive endpoints, one has

$$\tilde{G}_{\infty}(x, p|x_0) = \frac{e^{-\gamma(x-x_0)}}{\beta D \sinh(\beta L)} \times \begin{cases} \sinh(\beta \bar{x}_0) \sinh(\beta x) & (0 < x < x_0), \\ \sinh(\beta \bar{x}) \sinh(\beta x_0) & (x_0 < x < L), \end{cases} \quad (66)$$

where $\bar{x} = L - x$ and $\bar{x}_0 = L - x_0$. The Laplace-transformed probability flux density reads then

$$\tilde{j}_{\infty}(0, p|x_0) = \left(\mu \tilde{G}_{\infty}(x, p|x_0) + D \partial_x \tilde{G}_{\infty}(x, p|x_0) \right) \Big|_{x=0} = \frac{e^{\gamma x_0} \sinh(\beta \bar{x}_0)}{\sinh(\beta L)}, \quad (67)$$

$$\tilde{j}_{\infty}(L, p|x_0) = \left(\mu \tilde{G}_{\infty}(x, p|x_0) - D \partial_x \tilde{G}_{\infty}(x, p|x_0) \right) \Big|_{x=L} = \frac{e^{\gamma(x_0-L)} \sinh(\beta x_0)}{\sinh(\beta L)}. \quad (68)$$

Similarly, we have

$$\tilde{j}_{\infty}^{\prime}(0, p|x) = \left(D \partial_{x_0} \tilde{G}_{\infty}(x, p|x_0) \right) \Big|_{x_0=0} = \frac{e^{-\gamma x} \sinh(\beta \bar{x})}{\sinh(\beta L)}, \quad (69)$$

$$\tilde{j}_{\infty}^{\prime}(L, p|x) = \left(-D \partial_{x_0} \tilde{G}_{\infty}(x, p|x_0) \right) \Big|_{x_0=L} = \frac{e^{-\gamma(x-L)} \sinh(\beta x)}{\sinh(\beta L)}. \quad (70)$$

Expectedly, the functions $\tilde{j}_{\infty}(0, p|x_0)$ and $\tilde{j}_{\infty}^{\prime}(0, p|x_0)$ differ only by the sign of the drift (here, the sign of γ).

3.3. Propagators

According to equations (40) and (41), one has to project the probability flux densities onto the eigenfunctions of \mathcal{M}_p to get $V_n^{(p)}$ and $V_n^{\prime(p)}$. As the boundary consists of two endpoints, integrals are reduced to sums with two contributions:

$$\begin{aligned} V_{\pm}^{(p)}(x_0) &= v_{\pm}^{(p)}(0) \tilde{j}_{\infty}(0, p|x_0) + v_{\pm}^{(p)}(L) e^{\gamma L} \tilde{j}_{\infty}(L, p|x_0) \\ &= \frac{e^{\gamma x_0}}{\sinh(\beta L)} \left(v_{\pm}^{(p)}(0) \sinh(\beta \bar{x}_0) + v_{\pm}^{(p)}(L) \sinh(\beta x_0) \right), \\ V_{\pm}^{\prime(p)}(x) &= v_{\pm}^{(p)}(0) \tilde{j}_{\infty}^{\prime}(0, p|x) + v_{\pm}^{(p)}(L) e^{-\gamma L} \tilde{j}_{\infty}^{\prime}(L, p|x) \\ &= \frac{e^{-\gamma x}}{\sinh(\beta L)} \left(v_{\pm}^{(p)}(0) \sinh(\beta \bar{x}) + v_{\pm}^{(p)}(L) \sinh(\beta x) \right). \end{aligned}$$

As a consequence, equations (39) and (42) imply

$$\tilde{G}_q(x, p|x_0) = \tilde{G}_\infty(x, p|x_0) + \frac{1}{D} \left(\frac{V_+^{(p)}(x_0)V_+^{(p)}(x)}{q + \mu_+^{(p)}} + \frac{V_-^{(p)}(x_0)V_-^{(p)}(x)}{q + \mu_-^{(p)}} \right) \quad (71)$$

and

$$\tilde{P}(x, \ell, p|x_0) = \tilde{G}_\infty(x, p|x_0)\delta(\ell) + \frac{1}{D} \left(V_+^{(p)}(x_0)V_+^{(p)}(x)e^{-\ell\mu_+^{(p)}} + V_-^{(p)}(x_0)V_-^{(p)}(x)e^{-\ell\mu_-^{(p)}} \right). \quad (72)$$

Note that when the particle starts from one of the endpoints, the first term vanishes, and one also has $V_\pm^{(p)}(0) = v_\pm^{(p)}(0)$ and $V_\pm^{(p)}(L) = e^{\gamma L}v_\pm^{(p)}(L)$. While the Green's function $\tilde{G}_q(x, p|x_0)$ for partially reactive endpoints was known (and could be derived in a direct way, see appendix B), the explicit form (72) of the Laplace-transformed full propagator presents a new result. These expressions in the no drift limit are detailed in appendix C.

3.4. Mean boundary local time

Rewriting equation (46) explicitly as

$$\overline{V_\pm^{(p)}} = \frac{D\mu_\pm^{(p)}}{p} \left(v_\pm^{(p)}(0) + e^{-\gamma L}v_\pm^{(p)}(L) \right), \quad (73)$$

we get from equation (48) the Laplace transform of the mean boundary local time:

$$\int_0^\infty dt e^{-pt} \mathbb{E}_{x_0} \{ \ell_t \} = \frac{1}{p} \sum_{\pm} \frac{v_\pm^{(p)}(0) + e^{-\gamma L}v_\pm^{(p)}(L)}{\mu_\pm^{(p)}} \times \frac{e^{\gamma x_0}}{\sinh(\beta L)} \left(v_\pm^{(p)}(0) \sinh(\beta x_0) + v_\pm^{(p)}(L) \sinh(\beta x_0) \right), \quad (74)$$

where the sum contains only two terms. Note that higher-order moments of ℓ_t can be written in a similar way. Using the exact solution (74) in the Laplace domain, one can analyze the short-time and long-time behavior of the mean boundary local time. Here we only sketch the major points whereas the computational details are given in appendix D.

The long-time regime refers to the situation when a particle has enough time to explore the whole confining domain a number of times, i.e. $Dt \gg L^2$. This regime corresponds to the limit $p \rightarrow 0$, for which $\mu_+^{(p)} \approx 2\gamma \operatorname{ctanh}(\gamma L) + O(p)$ and $\mu_-^{(p)} \approx p \frac{\operatorname{tanh}(\gamma L)}{2\gamma D} + O(p^2)$. As the other 'ingredients' in equation (74) converge to finite limits as $p \rightarrow 0$ (and $\gamma \neq 0$), one deduces the long-time asymptotic behavior:

$$\mathbb{E}_{x_0} \{ \ell_t \} \simeq 2\gamma \operatorname{ctanh}(\gamma L)Dt + O(1) \quad (t \rightarrow \infty). \quad (75)$$

Expectedly, the long-time behavior does not depend on the starting point x_0 . In the no drift limit, $\gamma \rightarrow 0$, the constant in front of the leading term approaches $2D/L$, yielding

$$\mathbb{E}_{x_0} \{ \ell_t \} \simeq \frac{2Dt}{L} + O(1) \quad (t \rightarrow \infty), \quad (76)$$

in agreement with the general long-time behavior for ordinary diffusion in bounded domains [41]. The factor $\gamma \operatorname{ctanh}(\gamma L)$ is an even monotonously increasing function: whatever the sign of the drift, it tends to increase the mean boundary local time in the long-time limit by keeping the particle closer to the boundary and thus enhancing their encounters.

The behavior is totally different in the short-time limit. First, the initial position of the particle plays the crucial role. Indeed, the particle started in the bulk (i.e. $0 < x_0 < L$) needs some time for traveling to the boundary in order to make the very first encounter (i.e. to get $\ell_t > 0$). As a consequence, the mean $\mathbb{E}_{x_0}\{\ell_t\}$ vanishes exponentially fast as $t \rightarrow 0$ (see appendix D for details). In contrast, when the particle starts on the boundary, $\mathbb{E}_{x_0}\{\ell_t\}$ exhibits a power-law behavior. We derived the short-time asymptotic formula (D.5) for $\mathbb{E}_0\{\ell_t\}$ that can be written as

$$\mathbb{E}_0\{\ell_t\} \approx \frac{F(-\gamma\sqrt{Dt})}{\gamma} \quad (t \rightarrow 0), \tag{77}$$

with

$$F(x) = -\frac{1}{2}\text{erf}(x) + x^2(1 - \text{erf}(x)) - \frac{|x|e^{-x^2}}{\sqrt{\pi}}, \tag{78}$$

where $\text{erf}(x)$ is the error function. By introducing the time scale $t_\mu = 1/(D\gamma^2) = 4D/\mu^2$ associated to the drift, we can distinguish the cases of positive and negative drifts, as well as the limits of very short ($t \ll t_\mu$) and intermediate short ($t_\mu \ll t \ll L^2/D$) times.

- (a) For a positive drift (i.e. $\mu > 0$ and $\gamma < 0$), one has $F(x) \simeq -2x/\sqrt{\pi} + x^2 + O(x^3)$ as $x = |\gamma|\sqrt{Dt} \rightarrow 0$, and thus

$$\mathbb{E}_0\{\ell_t\} \approx \frac{2\sqrt{Dt}}{\sqrt{\pi}} - \frac{1}{2}|\mu|t \quad (t \ll t_\mu, \mu > 0). \tag{79}$$

The leading, \sqrt{t} -term remains unaffected by the drift, which enters in the next-order correction. In particular, one retrieves the result from [41] for restricted diffusion without drift. In turn, for intermediate short times $t \gg t_\mu$, one uses $F(x) \approx 1/2$ as $x \rightarrow \infty$ to get

$$\mathbb{E}_0\{\ell_t\} \approx \frac{D}{2|\mu|} \quad (t_\mu \ll t \ll L^2/D, \mu > 0). \tag{80}$$

In summary, a positive drift slightly diminishes the mean boundary local time via the next-order correction in equation (79), and then leads to a constant value controlled by $|\gamma|$, before reaching the long-time regime. This behavior agrees with the probabilistic picture, in which a positive drift facilitates the departure of the particle from the left endpoint x_0 . In a typical realization, the particle started from $x_0 = 0$ hits the left endpoint a number of times and then diffuses toward the right endpoint. The plateau in equation (80) corresponds, on average, to the passage from the left to the right endpoint, during which the boundary local time does not change.

- (b) For a negative drift (i.e. $\mu < 0$ and $\gamma > 0$), the situation is different. At very short times, one has $F(x) \simeq x^2 + O(x^3)$ as $x = -\gamma\sqrt{Dt} \rightarrow 0$ and thus

$$\mathbb{E}_0\{\ell_t\} \approx \frac{1}{2}|\mu|t \quad (t \ll t_\mu, \mu < 0). \tag{81}$$

Here, the linear slope, which is generally reminiscent of the long-time behavior, is controlled by the drift, which keeps the particle in the vicinity of the left endpoint. For intermediate short times, one has $F(x) \simeq 2x^2 + 1/2$ as $x \rightarrow -\infty$. Neglecting the constant $1/2$ in comparison to $2x^2$ in this limit, one gets

$$\mathbb{E}_0\{\ell_t\} \approx |\mu|t \quad (t_\mu \ll t \ll L^2/D, \mu < 0), \tag{82}$$

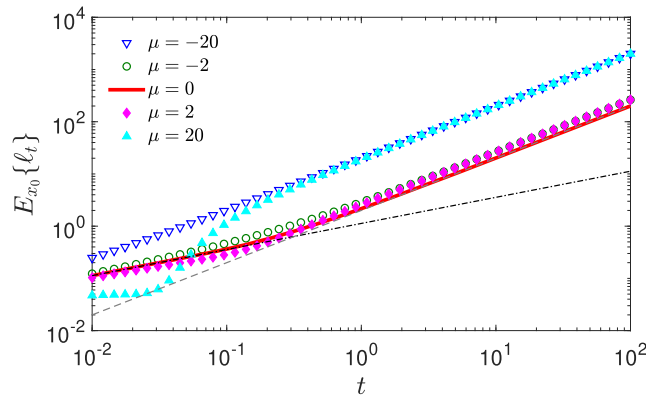


Figure 2. Mean boundary local time $\mathbb{E}_{x_0}\{\ell_t\}$ on the unit interval ($L = 1$), with $D = 1$, $x_0 = 0$, and five values of μ , as shown in the legend. Dashed and dash-dotted lines illustrate respectively the short-time relation (79) with $\mu = 0$ and the long-time relation (76) for the case without drift. $\mathbb{E}_{x_0}\{\ell_t\}$ was obtained via a numerical Laplace transform inversion by a modified Talbot algorithm (see appendix E).

i.e. the linear growth remains valid at intermediate times as well. Finally, at long times, the linear scaling is retrieved again, with the slope being controlled by the length of the interval (if the drift is not too strong).

Figure 2 illustrates the above picture. The red solid line presents the mean boundary local time $\mathbb{E}_0\{\ell_t\}$ for restricted diffusion without drift, which agrees well with both long-time and short-time asymptotic relations (76), (79). Four other curves plotted by symbols show $\mathbb{E}_0\{\ell_t\}$ in the presence of drift (with four different values of μ). At long times, the drift shifts the curves upwards in the loglog plot due the prefactor $\gamma \tanh(\gamma L)$ in front of t in equation (75). The effect is the same for both positive and negative drifts. At short times, we retrieve the asymptotic behavior described above by equations (79)–(82) for positive and negative drifts. In particular, one clearly sees the plateau region in the case $\mu = 20$. In turn, this region is not present for $\mu = 2$ because the time window of this regime, $t_\mu \ll t \ll L^2/D$, is empty, given that $t_\mu = L^2/D = 1$.

3.5. Distribution of the boundary local time

To get the distribution of the boundary local time ℓ_t , it is enough to integrate the full propagator over x . In fact, if $P(\circ, \ell, t|x_0)$ denotes the probability density of ℓ_t , its Laplace transform reads

$$\tilde{P}(\circ, \ell, p|x_0) = \tilde{S}_\infty(p|x_0)\delta(\ell) + \frac{1}{D} \left(V_+^{(p)}(x_0)\overline{V_+^{(p)}} e^{-\ell\mu_+^{(p)}} + V_-^{(p)}(x_0)\overline{V_-^{(p)}} e^{-\ell\mu_-^{(p)}} \right), \tag{83}$$

where

$$\tilde{S}_\infty(p|x_0) = \frac{1}{p} \left(1 - \frac{\sinh(\beta\bar{x}_0)e^{\gamma x_0} + \sinh(\beta x_0)e^{-\gamma\bar{x}_0}}{\sinh(\beta L)} \right). \tag{84}$$

For illustration purposes, we consider the situation when the particle is already on the boundary, so that there is no contribution from the first term in equation (83). As the problem is invariant under reflection with respect to the center of the interval (i.e. changing x_0 to $L - x_0$)

along with changing μ to $-\mu$, one can focus on the starting point $x_0 = 0$. Figure 3 illustrates the behavior of the probability density $P(\circ, \ell, t|0)$ of the boundary local time ℓ_t . According to equation (83), the Laplace transform of this function reaches a constant as $\ell \rightarrow 0$, and rapidly vanishes at large ℓ . These properties are preserved in time domain, even though the value of the constant at small ℓ depends on time t . As the short-time limit corresponds to $p \rightarrow \infty$, the value $\tilde{P}(\circ, 0, p|0)$ weakly depends on the drift, and so does $P(\circ, 0, t|0)$, as one can see on the panel (a) for $t = 0.01$. Expectedly, the distribution is shifted to the right (toward larger ℓ) by a negative drift which keeps the particle in the vicinity of the left endpoint and thus facilitates encounters. In contrast, a positive drift has the opposite effect. At an intermediate time $t = 0.1$ (panel (b)), the small- ℓ behavior of $P(\circ, \ell, t|0)$ is more sensitive to the drift, in particular, the constant plateau at $\ell \rightarrow 0$ is strongly attenuated by a strong negative drift ($\mu = -20$) because small values of ℓ are highly unlikely. A similar trend is also visible for strong positive drift ($\mu = 20$) which facilitates the passage to the right endpoint. Finally, at moderately long time $t = 1$ (panel (c)), there is almost no difference in the effect of positive and negative drifts. The distribution becomes peaked around the mean value at large drifts $\mu = \pm 20$.

To complete this section, we briefly discuss the probability density $p\tilde{P}(\circ, \ell, p|x_0)$ of the boundary local time ℓ_τ , which is stopped at a random time τ with an exponential distribution: $\mathbb{P}\{\tau > t\} = e^{-pt}$. Such a stopping time can describe restricted diffusion in a reactive medium, in which the particle can spontaneously disappear with the rate p ; alternatively, it can describe mortal walkers with a finite lifetime [54, 55]. In this setting, we are interested in the boundary local time at the death moment, i.e. how many times the particle encountered the boundary during its lifetime. According to equation (83), the probability density of ℓ_τ is simply a bi-exponential function, whose decay rates are controlled by the eigenvalues $\mu_\pm^{(p)}$. In this setting, equation (83) does not require an inverse Laplace transform anymore and thus allows for a complete, fully explicit and elementary study. We skip this analysis and illustrate the behavior of the probability density on figure 4. As previously, a negative drift keeps the particle near the left endpoint and enhances its encounters with that boundary, yielding higher probability for larger values of ℓ_τ . In turn, a strong positive drift results in two constant levels of the probability density: a higher plateau at small ℓ , which corresponds to encounters with the right endpoint, and a lower plateau at larger ℓ , which represents the contribution of encounters with the left endpoint (as in the case of the negative drift). In fact, when the particle leaves the left endpoint, it spends a considerable part of its lifetime to diffuse toward the right endpoint, during which the boundary local time does not change. As a consequence, one gets small ℓ_τ for such realizations. We note that the qualitative behavior for two considered reaction rates $p = 0.1$ and $p = 1$ is very similar, except that the decay at large ℓ is faster for $p = 1$ because the particles with the shorter lifetime get on average smaller ℓ_τ .

4. Discussion

In this paper, we extended the encounter-based approach developed in [8] to restricted diffusion with a gradient drift. This approach relies on the Langevin (or Skorokhod) stochastic differential equation that describes simultaneously the position of a particle and its boundary local time. Quite naturally, their joint probability density $P(\mathbf{x}, \ell, t|x_0)$, that we called the full propagator, appears to be the fundamental characteristics of restricted diffusion. This quantity is independent of surface reactions and thus properly describes the dynamics alone. In turn, the conventional propagator, which accounts for surface reactions through the Robin boundary condition, can then be deduced as the Laplace transform of $P(\mathbf{x}, \ell, t|x_0)$

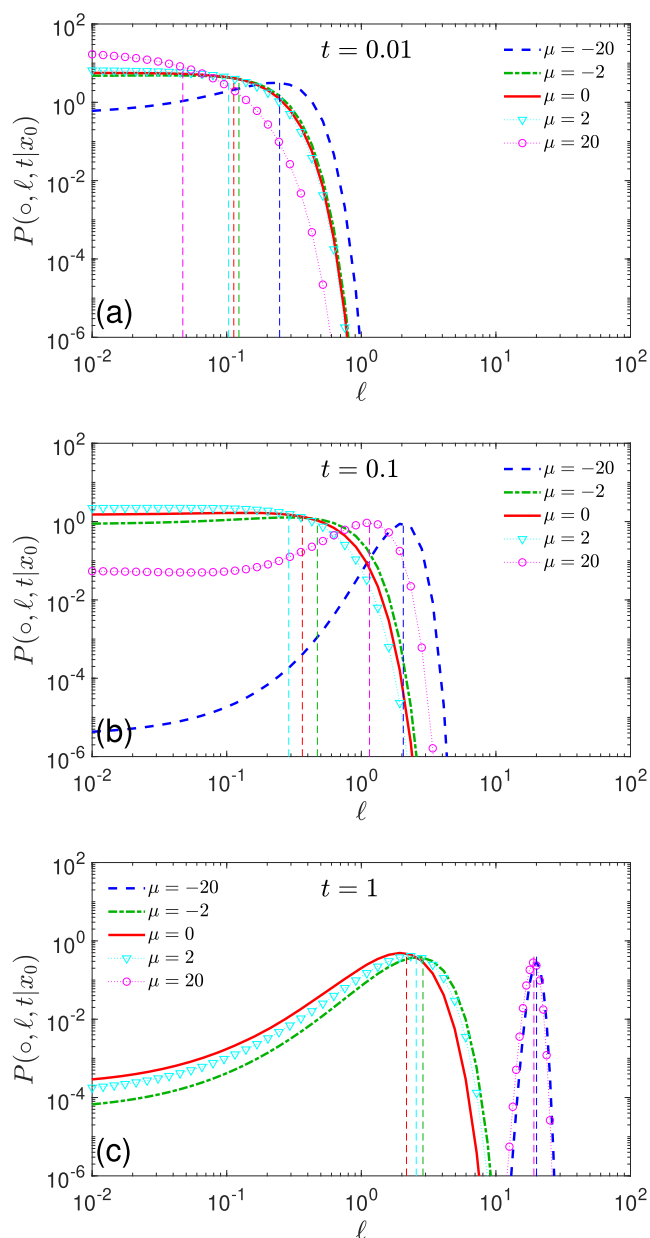


Figure 3. Probability density $P(\circ, \ell, t|x_0)$ of the boundary local time ℓ_t on the unit interval ($L = 1$), with $D = 1$, $x_0 = 0$, and five values of μ (given in the legend) and three values of t : (a) $t = 0.01$, (b) $t = 0.1$, and (c) $t = 1$. Vertical dashed lines indicate the corresponding mean boundary local times $\mathbb{E}_0\{\ell_t\}$. Both $P(\circ, \ell, t|x_0)$ and $\mathbb{E}_0\{\ell_t\}$ were obtained via a numerical Laplace transform inversion by a modified Talbot algorithm (see appendix E).

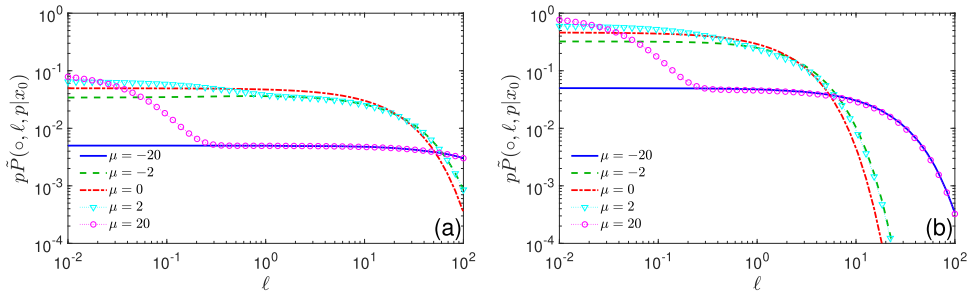


Figure 4. Probability density $\tilde{p}(\pi, \ell, p|x_0)$ of the boundary local time ℓ_τ (stopped at a random time τ exponentially distributed with rate p) on the unit interval ($L = 1$), with $D = 1$, five values of μ (given in the legend), and two values of the rate p : (a) $p = 0.1$ and (b) $p = 1$.

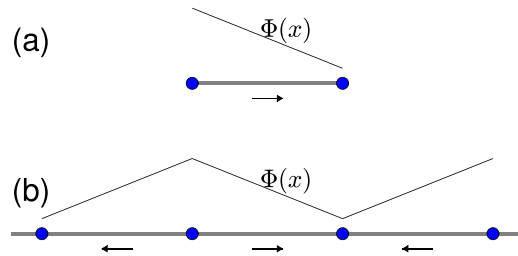


Figure 5. (a) An interval of length L with two reflecting endpoints and a linearly decreasing potential $\Phi(x)$ that describes a positive drift; (b) An infinite line with equally spaced discrete points $\{nL\}$ and a triangular periodic potential $\Phi(x)$ that describes alternating positive and negative drifts.

with respect to the boundary local time ℓ . This relation reflects the Bernoulli character of the surface reaction mechanism when the particle attempts to react at each encounter with equal probabilities and these trials are independent from each other. Most importantly, other surface reaction mechanisms can be implemented in a very similar way by replacing the exponential stopping condition. The disentanglement of the diffusive dynamics from surface reactions presents thus one of the major advantages of the encounter-based approach.

In order to derive a spectral decomposition for the Laplace-transformed full propagator, we introduced an appropriate Dirichlet-to-Neumann operator based on the symmetrized version of the Fokker–Planck operator. We illustrated the advantages of this approach in the case of restricted diffusion on an interval with a constant drift. In particular, we analyzed the distribution of the boundary local time and showed the effects of both positive and negative drifts at short and long times. We note that restricted diffusion on the interval $(0, L)$ with reflecting endpoints is equivalent to that on an infinite line and on a circle. As a consequence, the obtained exact formula for the distribution of the boundary local time can also describe (i) the boundary local time on discrete points $\{nL\}_{n \in \mathbb{Z}}$ equally spaced on an infinite line with a periodic triangular potential (see figure 5), and (ii) the boundary local time on an even number of equally spaced points on a circle.

Throughout the manuscript, the whole boundary was supposed to be reactive. In many applications, however, one deals with a reactive region $\mathcal{R} \subset \partial\Omega$ on otherwise inert impermeable boundary, and aims at finding the distribution of first-reaction times on that region. In this case, the Robin boundary condition (8) is replaced by mixed Robin–Neumann boundary condition

$$j_q(\mathbf{s}, t|\mathbf{x}_0) = \begin{cases} \kappa G_q(\mathbf{s}, t|\mathbf{x}_0) & (\mathbf{s} \in \mathcal{R}), \\ 0 & (\mathbf{s} \in \partial\Omega \setminus \mathcal{R}). \end{cases} \quad (85)$$

As discussed in [53], an extension of the encounter-based approach to this setting is straightforward. In fact, one focuses on the boundary local time on the reactive region \mathcal{R} , which is obtained by substituting $\partial\Omega$ by \mathcal{R} in equation (2). The former derivations remain valid, if the definition (36) of the Dirichlet-to-Neumann operator \mathcal{M}_p is generalized as

$$\mathcal{M}_p f = (\partial_n w + \phi(\mathbf{x})w)|_{\mathcal{R}}, \quad \text{with} \quad \begin{cases} (p - \bar{\mathcal{L}}_x)w = 0 & (\mathbf{x} \in \Omega), \\ w = f & (\mathbf{x} \in \mathcal{R}), \\ \partial_n w + \phi(\mathbf{x})w = 0 & (\mathbf{x} \in \partial\Omega \setminus \mathcal{R}). \end{cases} \quad (86)$$

In other words, the operator \mathcal{M}_p associates to a function f on the reactive region \mathcal{R} another function on \mathcal{R} , keeping the reflecting boundary condition for the solution w on the remaining inert region $\partial\Omega \setminus \mathcal{R}$. Examples of this extension for ordinary diffusion were given in [53]. As the reactive region does not need to be connected, the problem of multiple reactive sites can be treated in this framework. In addition, one can include an absorbing region $\mathcal{A} \subset \partial\Omega$ that kills the particle upon the first encounter. In this way, one can investigate surface reactions on \mathcal{R} for a sub-population of particles that avoid hitting \mathcal{A} . An implementation of this setting consists in adding the boundary condition $w = 0$ on \mathcal{A} in the definition (86) of the Dirichlet-to-Neumann operator (see further discussions in [57]). To get more subtle insights onto reactions on different reactive sites (e.g. competition between them), one can introduce the individual boundary local time on each site and look at their joint distribution [57]. However, appropriate spectral decompositions in this setting are yet unknown.

The proposed encounter-based approach can be further developed in different directions. On one hand, one can dwell on a rigorous proof of the spectral decompositions, on mathematical conditions for the boundary smoothness, on the spectral properties of the introduced extension of the Dirichlet-to-Neumann operator \mathcal{M}_p , and on their probabilistic interpretations. In particular, we assumed that \mathcal{M}_p is a self-adjoint operator with a discrete spectrum, without discussing eventual limitations on the drift $\boldsymbol{\mu}(\mathbf{x})$. Moreover, one can further extend the present approach to unbounded domains with a compact boundary (e.g. the exterior of a ball). While such an extension was already realized for diffusion without drift (see, e.g. [56]), some limitations on the drift $\boldsymbol{\mu}(\mathbf{x})$ can be expected to ensure the discrete spectrum of the Dirichlet-to-Neumann operator. Yet another mathematical direction is related to the asymptotic analysis of the narrow-escape problem when only a small fraction of the boundary is reactive. On the other hand, one can further explore the advantages of the encounter-based approach for various physical settings. For instance, one can consider the effect of local potentials near the boundary (such as, e.g. electrostatic repulsion or attractive interactions) onto the statistics of boundary encounters. One can consider other surface reaction mechanisms [8] and investigate how the drift may affect them. To some extent, such an approach can provide a microscopic model for so-called intermittent diffusions, in which a particle alternates diffusions in the bulk and on the surface [58–67]. Similarly, this approach may also help for studying diffusion with

reversible binding to the boundary, the so-called sticky boundary condition, when the particle stays on the boundary for a random waiting time and then unbinds to resume its bulk diffusion. The effects of this reversible binding onto reaction rates and first-passage times were thoroughly investigated for ordinary diffusion (see [68–72] and references therein), as well as for more sophisticated processes such as diffusion with stochastic resetting [73–76] or velocity jump processes [77–81]. Since binding to the boundary can be understood as a reaction event on that boundary, the binding time can be described as the first moment when the boundary local time exceeds an exponentially distributed threshold, as in equation (13). Changing the probability law for the random threshold allows one to incorporate more sophisticated binding mechanisms (see [8] for details). Curiously, the unbinding event implies resetting of the boundary local time.

Numerous advantages of the encounter-based approach urge for its extensions to even more general diffusion processes, in particular, with general space-dependent drift and volatility matrix. Such an extension would have to overcome two major difficulties.

- (a) When the diffusivity varies in the bulk, the reactivity parameter $q = \kappa/D$ becomes space-dependent as well. As a consequence, the probability of reaction at each encounter depends on the position of that encounter. This dependence would thus prohibit using the Laplace transform relation (16) between the full propagator and the conventional propagator. Following [44], one would thus need to introduce a functional of $q(X_t)$ to account for the cumulative effect of multiple reaction attempts (see also discussion in [57]). Note that a similar difficulty appears in the case of ordinary diffusion toward a heterogeneously reactive boundary, in which case the space-dependent reactivity κ renders q to be space-dependent as well [41].
- (b) Even if the diffusivity remains constant, an extension to a general drift becomes challenging. In fact, the Fokker–Planck operator can be reduced to a self-adjoint form with real eigenvalues only in the case of a gradient drift [82]. Even though an appropriate Dirichlet-to-Neumann operator can potentially be introduced in a more general case, such an operator is likely to be non-self-adjoint that would raise considerable challenges in the spectral analysis. Moreover, the numerical computation of the related spectral properties may also be difficult. Nevertheless, further mathematical works in this direction are expected to shed light onto more general diffusion-influenced reactions.

More generally, one can go beyond the framework of stochastic differential equations with Gaussian noises. In the simplest case of random walks on a lattice or a graph, the boundary local time is the number of visits of a given subset of vertices, which can be interpreted as partially reactive sites or localized traps. Szabo *et al* showed how to express the related propagator in terms of the propagator without trapping [83]. This concept was recently extended to more general random walks [84]. Another interesting extension concerns diffusion processes with stochastic resetting [73–76], which can be implemented either for the position, or for the boundary local time, or for both processes. The renewal character of such resets may allow getting rather explicit results in the Laplace domain. Moreover, the main idea of the encounter-based approach can be potentially applied to other examples of stochastic dynamics such as, e.g. velocity jump processes (including run-and-tumble motion) [77–81] and continuous-time random walks (including even Lévy flights). However, one would need to properly define the boundary local time (or its analog), as well as an appropriate governing operator (such as the Dirichlet-to-Neumann operator), whose spectral properties would determine the full propagator. Feasibility, mathematical rigor and practical value of such extensions are still open.

Acknowledgments

The author acknowledges the Alexander von Humboldt Foundation for support within a Bessel Prize award.

Data availability statement

All data that support the findings of this study are included within the article (and any supplementary files).

Appendix A. Auxiliary relation

In this appendix, we obtain equation (46) by extending the derivation from [41].

First, the integral of equation (18) over $\mathbf{x} \in \Omega$ yields

$$\begin{aligned} p \int_{\Omega} d\mathbf{x} \tilde{G}_{\infty}(\mathbf{x}, p|\mathbf{x}_0) &= 1 + \int_{\Omega} d\mathbf{x} (D\Delta - (\nabla\mu))\tilde{G}_{\infty}(\mathbf{x}, p|\mathbf{x}_0) \\ &= 1 + \int_{\partial\Omega} d\mathbf{x} D\partial_n \tilde{G}_{\infty}(\mathbf{x}, p|\mathbf{x}_0). \end{aligned}$$

Taking the normal derivative with respect to \mathbf{x}_0 at $\mathbf{x}_0 = s_0 \in \partial\Omega$ and multiplying by $-D/p$, we get

$$\int_{\Omega} d\mathbf{x} \tilde{j}_{\infty}^j(s_0, p|\mathbf{x}) = -\frac{D}{p} \int_{\partial\Omega} d\mathbf{x} D(\partial_{n_0} \partial_n \tilde{G}_{\infty}(\mathbf{x}, p|\mathbf{x}_0))|_{\mathbf{x}_0=s_0}. \quad (\text{A.1})$$

Our intention is to exchange the order of normal derivatives in the right-hand side in order to get $\tilde{j}_{\infty}^j(s_0, p|\mathbf{x})$. However, as this function is singular in the vicinity of $\mathbf{x} \approx s_0$, one cannot simply exchange the order. To proceed, we use equation (26) and evaluate the following derivatives:

$$\begin{aligned} \partial_{n_0} \partial_n \tilde{G}_{\infty}(\mathbf{x}, p|\mathbf{x}_0) &= \partial_{n_0} \partial_n e^{-\frac{1}{2}\Phi(\mathbf{x}) + \frac{1}{2}\Phi(\mathbf{x}_0)} \tilde{g}_{\infty}(\mathbf{x}, p|\mathbf{x}_0) \\ &= e^{-\frac{1}{2}\Phi(\mathbf{x}) + \frac{1}{2}\Phi(\mathbf{x}_0)} \left(-\phi(\mathbf{x}) \partial_{n_0} \tilde{g}_{\infty}(\mathbf{x}, p|\mathbf{x}_0) + \partial_{n_0} \partial_n \tilde{g}_{\infty}(\mathbf{x}, p|\mathbf{x}_0) \right), \\ \partial_n \partial_{n_0} \tilde{G}_{\infty}(\mathbf{x}, p|\mathbf{x}_0) &= \partial_n \partial_{n_0} e^{-\frac{1}{2}\Phi(\mathbf{x}) + \frac{1}{2}\Phi(\mathbf{x}_0)} \tilde{g}_{\infty}(\mathbf{x}, p|\mathbf{x}_0) \\ &= e^{-\frac{1}{2}\Phi(\mathbf{x}) + \frac{1}{2}\Phi(\mathbf{x}_0)} \left(\phi(\mathbf{x}_0) \partial_n \tilde{g}_{\infty}(\mathbf{x}, p|\mathbf{x}_0) + \partial_n \partial_{n_0} \tilde{g}_{\infty}(\mathbf{x}, p|\mathbf{x}_0) \right). \end{aligned}$$

Since the function $\tilde{g}_{\infty}(\mathbf{x}, p|\mathbf{x}_0)$ is symmetric, one can exchange the order of normal derivatives. In addition, one has

$$\begin{aligned} \tilde{j}_{\infty}^j(\mathbf{x}, p|\mathbf{x}_0) &= -D\partial_n \left(e^{-\frac{1}{2}\Phi(\mathbf{x}) + \frac{1}{2}\Phi(\mathbf{x}_0)} \tilde{g}_{\infty}(\mathbf{x}, p|\mathbf{x}_0) \right) \\ &= \phi(\mathbf{x}) D\tilde{G}_{\infty}(\mathbf{x}, p|\mathbf{x}_0) - D e^{-\frac{1}{2}\Phi(\mathbf{x}) + \frac{1}{2}\Phi(\mathbf{x}_0)} \partial_n \tilde{g}_{\infty}(\mathbf{x}, p|\mathbf{x}_0), \\ \tilde{j}_{\infty}^j(\mathbf{x}_0, p|\mathbf{x}) &= -D\partial_{n_0} \left(e^{-\frac{1}{2}\Phi(\mathbf{x}) + \frac{1}{2}\Phi(\mathbf{x}_0)} \tilde{g}_{\infty}(\mathbf{x}, p|\mathbf{x}_0) \right) \\ &= -\phi(\mathbf{x}_0) D\tilde{G}_{\infty}(\mathbf{x}, p|\mathbf{x}_0) - D e^{-\frac{1}{2}\Phi(\mathbf{x}) + \frac{1}{2}\Phi(\mathbf{x}_0)} \partial_{n_0} \tilde{g}_{\infty}(\mathbf{x}, p|\mathbf{x}_0). \end{aligned}$$

Combining these relations and noting that $\tilde{j}_\infty(\mathbf{x}, p|\mathbf{x}_0) = \tilde{j}'_\infty(\mathbf{x}_0, p|\mathbf{x}) = \delta(\mathbf{x} - \mathbf{x}_0)$ when both \mathbf{x} and \mathbf{x}_0 belong to the boundary $\partial\Omega$, we get

$$\partial_{n_0}\partial_n\tilde{G}_\infty(\mathbf{x}, p|\mathbf{x}_0) - \partial_n\partial_{n_0}\tilde{G}_\infty(\mathbf{x}, p|\mathbf{x}_0) = \frac{\phi(\mathbf{x}) + \phi(\mathbf{x}_0)}{D}\delta(\mathbf{x} - \mathbf{x}_0). \tag{A.2}$$

This relation allows us to rewrite equation (A.1) as

$$\int_\Omega d\mathbf{x} \tilde{j}'_\infty(\mathbf{s}_0, p|\mathbf{x}) = \frac{D}{p} \int_{\partial\Omega} d\mathbf{x} (\partial_n \tilde{j}'_\infty(\mathbf{s}_0, p|\mathbf{x})) - \frac{2D\phi(\mathbf{s}_0)}{p}. \tag{A.3}$$

We multiply both sides of this equation by $e^{-\frac{1}{2}\Phi(\mathbf{s}_0)} f(\mathbf{s}_0)$ with a suitable function $f(\mathbf{s}_0)$ and integrate over $\mathbf{s}_0 \in \partial\Omega$:

$$\begin{aligned} & \int_{\partial\Omega} d\mathbf{s}_0 e^{-\frac{1}{2}\Phi(\mathbf{s}_0)} f(\mathbf{s}_0) \int_\Omega d\mathbf{x} \tilde{j}'_\infty(\mathbf{s}_0, p|\mathbf{x}) \\ &= \frac{D}{p} \int_{\partial\Omega} d\mathbf{s}_0 e^{-\frac{1}{2}\Phi(\mathbf{s}_0)} f(\mathbf{s}_0) \left\{ \int_{\partial\Omega} d\mathbf{s} (\partial_n \tilde{j}'_\infty(\mathbf{s}_0, p|\mathbf{s})) - 2\phi(\mathbf{s}_0) \right\}. \end{aligned} \tag{A.4}$$

Our aim is to show that the right-hand side can be represented via the Dirichlet-to-Neumann operator. For this purpose, we note that the solution of the equation $(p - \tilde{\mathcal{L}})u = 0$ with Dirichlet boundary condition $u = f$ on $\partial\Omega$ can be written as

$$\begin{aligned} u(\mathbf{x}) &= \int_\Omega d\mathbf{x}_0 [u(\mathbf{x}_0)(p - \tilde{\mathcal{L}}_{\mathbf{x}_0})\tilde{g}_\infty(\mathbf{x}, p|\mathbf{x}_0) - \tilde{g}_\infty(\mathbf{x}, p|\mathbf{x}_0)(p - \tilde{\mathcal{L}}_{\mathbf{x}_0})u(\mathbf{x}_0)] \\ &= \int_{\partial\Omega} d\mathbf{x}_0 u(\mathbf{x}_0)(-D\partial_{n_0}\tilde{g}_\infty(\mathbf{x}, p|\mathbf{x}_0)) \\ &= \int_{\partial\Omega} d\mathbf{x}_0 u(\mathbf{x}_0) \left(-D\partial_{n_0} e^{\frac{1}{2}\Phi(\mathbf{x}) - \frac{1}{2}\Phi(\mathbf{x}_0)} \tilde{G}_\infty(\mathbf{x}, p|\mathbf{x}_0) \right) \\ &= \int_{\partial\Omega} d\mathbf{s}_0 f(\mathbf{s}_0) e^{\frac{1}{2}\Phi(\mathbf{x}) - \frac{1}{2}\Phi(\mathbf{s}_0)} \tilde{j}'_\infty(\mathbf{s}_0, p|\mathbf{x}). \end{aligned}$$

As a consequence, the action of the Dirichlet-to-Neumann operator is

$$\begin{aligned} (\mathcal{M}_p f)(\mathbf{s}) &= \phi(\mathbf{s})f(\mathbf{s}) + (\partial_n u)_{\mathbf{x}=\mathbf{s}} \\ &= \phi(\mathbf{s})f(\mathbf{s}) + \int_{\partial\Omega} d\mathbf{s}_0 f(\mathbf{s}_0) e^{-\frac{1}{2}\Phi(\mathbf{s}_0)} \partial_n \left(e^{\frac{1}{2}\Phi(\mathbf{x})} \tilde{j}'_\infty(\mathbf{s}_0, p|\mathbf{x}) \right) |_{\mathbf{x}=\mathbf{s}} \\ &= \phi(\mathbf{s})f(\mathbf{s}) + \int_{\partial\Omega} d\mathbf{s}_0 f(\mathbf{s}_0) e^{-\frac{1}{2}\Phi(\mathbf{s}_0)} e^{\frac{1}{2}\Phi(\mathbf{s})} \left[\underbrace{\phi(\mathbf{s})\tilde{j}'_\infty(\mathbf{s}_0, p|\mathbf{s})}_{=\delta(\mathbf{s}-\mathbf{s}_0)} + (\partial_n \tilde{j}'_\infty(\mathbf{s}_0, p|\mathbf{x})) |_{\mathbf{x}=\mathbf{s}} \right] \\ &= 2\phi(\mathbf{s})f(\mathbf{s}) + \int_{\partial\Omega} d\mathbf{s}_0 f(\mathbf{s}_0) e^{-\frac{1}{2}\Phi(\mathbf{s}_0)} e^{\frac{1}{2}\Phi(\mathbf{s})} (\partial_n \tilde{j}'_\infty(\mathbf{s}_0, p|\mathbf{x})) |_{\mathbf{x}=\mathbf{s}}. \end{aligned}$$

This relation allows us to represent the integral over s_0 in the right-hand side of equation (A.4) in terms of \mathcal{M}_p :

$$\int_{\partial\Omega} ds_0 e^{-\frac{1}{2}\Phi(s_0)} f(s_0) \int_{\Omega} dx \tilde{j}_{\infty}^j(s_0, p|x) = \frac{D}{p} \left\{ \int_{\partial\Omega} ds e^{-\frac{1}{2}\Phi(s)} e^{\frac{1}{2}\Phi(s)} \underbrace{\int_{\partial\Omega} ds_0 e^{-\frac{1}{2}\Phi(s_0)} f(s_0) (\partial_n \tilde{j}_{\infty}^j(s_0, p|s))}_{=(\mathcal{M}_p f)(s) - 2\phi(s)f(s)} - 2 \int_{\partial\Omega} ds_0 e^{-\frac{1}{2}\Phi(s_0)} f(s_0) \phi(s_0) \right\},$$

i.e.

$$\int_{\partial\Omega} ds_0 e^{-\frac{1}{2}\Phi(s_0)} f(s_0) \int_{\Omega} dx \tilde{j}_{\infty}^j(s_0, p|x) = \frac{D}{p} \int_{\partial\Omega} ds e^{-\frac{1}{2}\Phi(s)} (\mathcal{M}_p f)(s). \tag{A.5}$$

This relation holds for any suitable function $f(s)$ on the boundary. Setting $f(s) = v_n^{(p)}(s)$ to be an eigenfunction of \mathcal{M}_p , one gets immediately

$$\begin{aligned} \overline{V_n^{(p)}} &= \int_{\Omega} dx \int_{\partial\Omega} ds_0 e^{-\frac{1}{2}\Phi(s_0)} v_n^{(p)}(s_0) \tilde{j}_{\infty}^j(s_0, p|x) \\ &= \frac{D}{p} \mu_n^{(p)} \int_{\partial\Omega} ds e^{-\frac{1}{2}\Phi(s)} v_n^{(p)}(s). \end{aligned} \tag{A.6}$$

Appendix B. Green’s functions on the interval

Even though many Green’s functions on the interval are known (see, e.g. [85]), we provide here the main steps of the derivation for the Fokker–Planck operator $\mathcal{L} = D\partial_x^2 - \mu\partial_x$ for completeness.

We start with the most general case of Robin boundary conditions at 0 and L , with two different reactivities q_1 and q_2 . A general solution of the equation $(p - \mathcal{L})u = 0$ reads $u(x) = c_+ e^{\alpha_+ x} + c_- e^{\alpha_- x}$, with

$$\alpha_{\pm} = \frac{\mu}{2D} \pm \sqrt{\frac{p}{D} + \frac{\mu^2}{4D^2}}, \tag{B.1}$$

and two arbitrary coefficients c_{\pm} . As usual, one searches for the solution of the equation (18) in the form

$$\tilde{G}_{q_1, q_2}(x, p|x_0) = \begin{cases} A [(1 - h_1 \alpha_-) e^{\alpha_+ x} - (1 - h_1 \alpha_+) e^{\alpha_- x}] & (0 < x < x_0), \\ B [(1 + h_2 \alpha_-) e^{\alpha_+ (x-L)} - (1 + h_2 \alpha_+) e^{\alpha_- (x-L)}] & (x_0 < x < L), \end{cases} \tag{B.2}$$

that satisfies the boundary condition (18) at both endpoints:

$$(-\partial_x + q_1 + \mu/D) \tilde{G}_{q_1, q_2}(x, p|x_0) = 0 \quad (x = 0), \tag{B.3}$$

$$(\partial_x + q_2 - \mu/D) \tilde{G}_{q_1, q_2}(x, p|x_0) = 0 \quad (x = L), \tag{B.4}$$

where we set $h_1 = 1/(q_1 + \mu/D)$ and $h_2 = 1/(q_2 - \mu/D)$. The unknown coefficients A and B are then determined by requiring the continuity of $\tilde{G}_{q_1, q_2}(x, p|x_0)$ at $x = x_0$ and the drop of the derivative by $-1/D$ (i.e. $[\partial_x \tilde{G}_{q_1, q_2}(x, p|x_0)]_{x=x_0+\epsilon} - [\partial_x \tilde{G}_{q_1, q_2}(x, p|x_0)]_{x=x_0-\epsilon} \rightarrow -1/D$ as $\epsilon \rightarrow 0$):

$$A = \frac{e^{\gamma x_0} [(1 - h_2 \gamma) \sinh(\beta \bar{x}_0) + \beta h_2 \cosh(\beta \bar{x}_0)]}{2\beta D [\sinh(\beta L)(1 + \gamma(h_1 - h_2)) + (\beta^2 - \gamma^2)h_1 h_2 + \cosh(\beta L)\beta(h_1 + h_2)]}, \tag{B.5}$$

$$B = -\frac{e^{\gamma(x_0-L)} [(1 + h_1 \gamma) \sinh(\beta x_0) + \beta h_1 \cosh(\beta x_0)]}{2\beta D [\sinh(\beta L)(1 + \gamma(h_1 - h_2)) + (\beta^2 - \gamma^2)h_1 h_2 + \cosh(\beta L)\beta(h_1 + h_2)]}, \tag{B.6}$$

where we used the former notations $\gamma = -\mu/(2D)$, $\beta = \sqrt{p/D + \gamma^2}$, and $\bar{x}_0 = L - x_0$. One can also write

$$\tilde{G}_{q_1, q_2}(x, p|x_0) = \begin{cases} 2Ae^{-\gamma x} [(1 + h_1 \gamma) \sinh(\beta x) + h_1 \beta \cosh(\beta x)] & (0 < x < x_0), \\ -2Be^{-\gamma(x-L)} [(1 - h_2 \gamma) \sinh(\beta \bar{x}) + h_2 \beta \cosh(\beta \bar{x})] & (x_0 < x < L), \end{cases}$$

with $\bar{x} = L - x$. Setting

$$U(x) = (1 + h_1 \gamma) \sinh(\beta x) + \beta h_1 \cosh(\beta x), \tag{B.7}$$

$$V(x) = (1 - h_2 \gamma) \sinh(\beta(L - x)) + \beta h_2 \cosh(\beta(L - x)), \tag{B.8}$$

$$C = \frac{1}{\beta D [\sinh(\beta L)(1 + \gamma(h_1 - h_2)) + (\beta^2 - \gamma^2)h_1 h_2 + \cosh(\beta L)\beta(h_1 + h_2)]}, \tag{B.9}$$

one can finally get

$$\tilde{G}_{q_1, q_2}(x, p|x_0) = Ce^{-\gamma(x-x_0)} \begin{cases} U(x)V(x_0) & (0 < x < x_0), \\ U(x_0)V(x) & (x_0 < x < L). \end{cases} \tag{B.10}$$

In the particular case of equal reactivities, $q_1 = q_2 = q$, one has

$$\begin{aligned} U(x) &= \frac{\hat{U}(x)}{q - 2\gamma}, & \hat{U}(x) &= (q - \gamma) \sinh(\beta x) + \beta \cosh(\beta x), \\ V(x) &= \frac{\hat{V}(x)}{q + 2\gamma}, & \hat{V}(x) &= (q + \gamma) \sinh(\beta(L - x)) + \beta \cosh(\beta(L - x)), \\ C &= \frac{\hat{C}}{q^2 - 4\gamma^2}, & \hat{C} &= \frac{1}{\beta D \sinh(\beta L) (q^2 + 2\beta \operatorname{ctanh}(\beta L)q + \beta^2 - \gamma^2)}. \end{aligned}$$

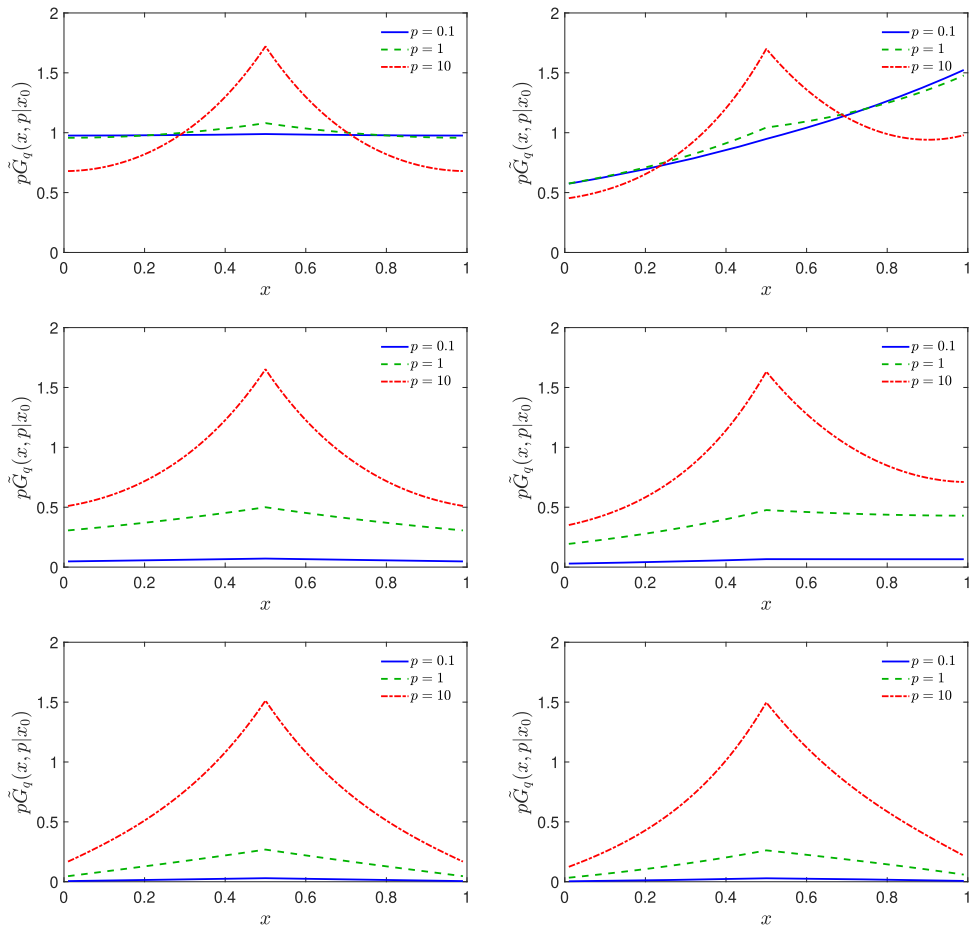


Figure B1. Green’s function $\tilde{G}_q(x, p|x_0)$ (multiplied by p) on the unit interval ($L = 1$), with $D = 1$, $x_0 = 0.5$, several values of p . Six panels correspond to $\mu = 0$ (left column) and $\mu = 1$ (right right) and $q = 10^{-3}$ (top row), $q = 1$ (middle row), and $q = 10$ (bottom row).

More explicitly, one gets

$$\begin{aligned} \tilde{G}_q(x, p|x_0) &= e^{-\gamma(x-x_0)} \frac{\sinh(\beta\bar{x}_0) \sinh(\beta x)}{\beta D \sinh(\beta L)} \\ &\times \frac{q^2 + q\beta(\operatorname{ctanh}(\beta\bar{x}_0) + \operatorname{ctanh}(\beta x)) - (\gamma - \beta\operatorname{ctanh}(\beta x))(\gamma + \beta\operatorname{ctanh}(\beta\bar{x}_0))}{q^2 + 2\beta\operatorname{ctanh}(\beta L)q + \beta^2 - \gamma^2} \end{aligned}$$

for $0 < x < x_0$, and

$$\begin{aligned} \tilde{G}_q(x, p|x_0) &= e^{-\gamma(x-x_0)} \frac{\sinh(\beta\bar{x}) \sinh(\beta x_0)}{\beta D \sinh(\beta L)} \\ &\times \frac{q^2 + q\beta(\operatorname{ctanh}(\beta\bar{x}) + \operatorname{ctanh}(\beta x_0)) - (\gamma - \beta\operatorname{ctanh}(\beta x_0))(\gamma + \beta\operatorname{ctanh}(\beta\bar{x}))}{q^2 + 2\beta\operatorname{ctanh}(\beta L)q + \beta^2 - \gamma^2} \end{aligned}$$

for $x_0 < x < L$. Considering this expression as a function q , one can decompose it into the sum of partial fractions and then perform the inverse Laplace transform with respect to q in order to get the full propagator. In this way, one can re-derive the general spectral decomposition.

Figure B1 illustrates the behavior of the Green’s function $\tilde{G}_q(x, p|x_0)$ (for visual convenience, this function is multiplied by p ; in fact, for $q = 0$, the integral of this function over x is equal to $1/p$). When $\mu = 1$, the right wing of $\tilde{G}_q(x, p|x_0)$ is higher, as the positive drift facilitates diffusion to the right.

Appendix C. No drift limit

In this Appendix, we briefly describe how the results of section 3 are simplified in the no drift limit.

In the limit $\mu \rightarrow 0$, the eigenvalues of the Dirichlet-to-Neumann operator tend to

$$\mu_{\pm}^{(p)} = \frac{\beta(\cosh(\beta L) \pm 1)}{\sinh(\beta L)} \quad \text{with} \quad \beta = \sqrt{p/D}, \tag{C.1}$$

while the eigenvectors tend to

$$v_{\pm}^{(p)} = \frac{1}{\sqrt{2}} \begin{pmatrix} 1 \\ \mp 1 \end{pmatrix}, \tag{C.2}$$

so that

$$V_{\pm}^{(p)}(x) = V_{\pm}^{(p)\prime}(x) = \frac{\sinh(\beta \bar{x}) \mp \sinh(\beta x)}{\sqrt{2} \sinh(\beta L)}. \tag{C.3}$$

In this way, we retrieve the Laplace-transformed full propagator for ordinary diffusion without drift,¹ first derived in [57]

$$\begin{aligned} \tilde{P}(x, \ell, p|x_0) &= \tilde{G}_{\infty}(x, p|x_0)\delta(\ell) + \frac{e^{-\ell\beta \operatorname{ctanh}(\beta L)}}{D} \\ &\times \left\{ \frac{\sinh(\beta \bar{x}_0) \sinh(\beta \bar{x}) + \sinh(\beta x_0) \sinh(\beta x)}{\sinh^2(\beta L)} \right. \\ &\times \cosh\left(\frac{\beta \ell}{\sinh(\beta L)}\right) + \frac{\sinh(\beta \bar{x}_0) \sinh(\beta x) + \sinh(\beta x_0) \sinh(\beta \bar{x})}{\sinh^2(\beta L)} \\ &\left. \times \sinh\left(\frac{\beta \ell}{\sinh(\beta L)}\right) \right\}. \end{aligned} \tag{C.4}$$

The marginal probability density of the boundary local time in the Laplace domain reads

$$\tilde{P}(\circ, \ell, p|x_0) = \tilde{S}_{\infty}(p|x_0)\delta(\ell) + \underbrace{\frac{\cosh(\beta L) - 1}{\beta \sinh(\beta L)}}_{= \frac{\tanh(\beta L/2)}{\beta}} \frac{\sinh(\beta x_0) + \sinh(\beta \bar{x}_0)}{\sinh(\beta L)} \frac{e^{-\beta \tanh(\beta L/2)\ell}}{D}. \tag{C.5}$$

¹ There is a misprint in the expression (A.7) from [57]: the sign minus in front of the second term should be replaced by plus, as in equation (C.4).

Appendix D. Asymptotic behavior

In this Appendix, we provide technical details for the asymptotic analysis of the short-time and long-time regimes, which correspond to the large- p and small- p limits in the Laplace domain, respectively.

D.1. Short-time behavior

Under the condition $L\sqrt{p/D} \gg 1$, we get $\beta L \gg 1$ and thus find $\mu_{\pm}^{(p)} \approx \beta \pm |\gamma|$, with exponentially small corrections. Similarly, we have $v_{+}^{(p)} \approx (1, 0)^{\dagger}$ and $v_{-}^{(p)} \approx (0, 1)^{\dagger}$ for $\mu > 0$, whereas the opposite relations hold for $\mu < 0$, namely, $v_{+}^{(p)} \approx (0, 1)^{\dagger}$ and $v_{-}^{(p)} \approx (1, 0)^{\dagger}$. As a consequence, we get

$$V_{+}^{(p)}(x_0) \approx e^{\gamma x_0 - \beta x_0}, \quad V_{-}^{(p)}(x_0) \approx e^{\gamma x_0 - \beta \bar{x}_0} \quad (\mu > 0), \quad (\text{D.1})$$

and

$$V_{+}^{(p)}(x_0) \approx e^{\gamma x_0 - \beta \bar{x}_0}, \quad V_{-}^{(p)}(x_0) \approx e^{\gamma x_0 - \beta x_0} \quad (\mu < 0). \quad (\text{D.2})$$

Substituting these expressions into equation (48), we get

$$\int_0^{\infty} dt e^{-pt} \mathbb{E}_{x_0} \{ \ell_t \} \approx \frac{1}{p} \left(\frac{e^{-(\beta-\gamma)x_0}}{\beta-\gamma} + \frac{e^{-(\beta+\gamma)(L-x_0)}}{\beta+\gamma} \right), \quad (\text{D.3})$$

whatever the sign of μ . Using the identity

$$\int_0^{\infty} dt e^{-pt} e^{-a^2/(4t)} \left(\frac{1}{\sqrt{\pi t}} - b \operatorname{erfcx} \left(\frac{a}{2\sqrt{t}} + b\sqrt{t} \right) \right) = \frac{e^{-a\sqrt{p}}}{\sqrt{p} + b} \quad (\text{D.4})$$

(here $\operatorname{erfcx}(x) = e^{x^2}(1 - \operatorname{erf}(x))$ is the scaled complementary error function), the inverse Laplace transform of equation (D.3) reads

$$\begin{aligned} \mathbb{E}_{x_0} \{ \ell_t \} &\approx \int_0^t dt' e^{-D\gamma^2 t'} \left\{ e^{\gamma x_0} \left[e^{-x_0^2/(4Dt')} \left(\frac{\sqrt{D}}{\sqrt{\pi t'}} + \gamma D \operatorname{erfcx} \left(\frac{x_0}{\sqrt{4Dt'}} - \gamma\sqrt{Dt'} \right) \right) \right] \right. \\ &\quad \left. + e^{\gamma(x_0-L)} \left[e^{-(L-x_0)^2/(4Dt')} \left(\frac{\sqrt{D}}{\sqrt{\pi t'}} - \gamma D \operatorname{erfcx} \left(\frac{L-x_0}{\sqrt{4Dt'}} + \gamma\sqrt{Dt'} \right) \right) \right] \right\} \\ &\approx \int_0^t dt' \left\{ e^{\gamma x_0} \left[e^{-D\gamma^2 t'} e^{-x_0^2/(4Dt')} \frac{\sqrt{D}}{\sqrt{\pi t'}} + \gamma D e^{-\gamma x_0} \operatorname{erfc} \left(\frac{x_0}{\sqrt{4Dt'}} - \gamma\sqrt{Dt'} \right) \right] \right. \\ &\quad \left. + e^{-\gamma(L-x_0)} \left[e^{-D\gamma^2 t'} e^{-(L-x_0)^2/(4Dt')} \frac{\sqrt{D}}{\sqrt{\pi t'}} - \gamma D e^{\gamma(L-x_0)} \operatorname{erfc} \left(\frac{L-x_0}{\sqrt{4Dt'}} + \gamma\sqrt{Dt'} \right) \right] \right\}. \end{aligned}$$

Using the identity

$$\int_0^t dt' \frac{e^{-at'-b/t'}}{\sqrt{t'}} = \frac{\sqrt{\pi}}{2\sqrt{a}} \left(e^{2\sqrt{ab}} \left(\operatorname{erf}(\sqrt{at} + \sqrt{b/t}) - 1 \right) + e^{-2\sqrt{ab}} \left(\operatorname{erf}(\sqrt{at} - \sqrt{b/t}) + 1 \right) \right),$$

we get

$$\begin{aligned} \mathbb{E}_{x_0} \{ \ell_t \} &\approx \frac{e^{\gamma x_0}}{2|\gamma|} \left[-e^{|\gamma|x_0} \operatorname{erfc}(x_0/\sqrt{4Dt} + |\gamma|\sqrt{Dt}) + e^{-|\gamma|x_0} \operatorname{erfc}(x_0/\sqrt{4Dt} - |\gamma|\sqrt{Dt}) \right] \\ &+ \frac{e^{-\gamma \bar{x}_0}}{2|\gamma|} \left[-e^{|\gamma|\bar{x}_0} \operatorname{erfc}(\bar{x}_0/\sqrt{4Dt} + |\gamma|\sqrt{Dt}) + e^{-|\gamma|\bar{x}_0} \operatorname{erfc}(\bar{x}_0/\sqrt{4Dt} - |\gamma|\sqrt{Dt}) \right] \\ &+ \gamma D \int_0^t dt' \left\{ \operatorname{erfc} \left(\frac{x_0}{\sqrt{4Dt'}} - \gamma\sqrt{Dt'} \right) - \operatorname{erfc} \left(\frac{\bar{x}_0}{\sqrt{4Dt'}} + \gamma\sqrt{Dt'} \right) \right\}. \end{aligned}$$

In particular, for $x_0 = 0$, we get after simplifications

$$\mathbb{E}_0 \{ \ell_t \} \approx \frac{1}{\gamma} \left(\frac{\operatorname{erf}(\gamma\sqrt{Dt})}{2} + \gamma^2 Dt \operatorname{erfc}(-\gamma\sqrt{Dt}) - \frac{|\gamma|\sqrt{Dt}}{\sqrt{\pi}} e^{-D\gamma^2 t} \right). \quad (\text{D.5})$$

D.2. Long-time behavior

Let us consider the case $\gamma \neq 0$. In the limit $p \rightarrow 0$, we get up to $O(p^2)$:

$$\begin{aligned} \beta &\approx |\gamma| + \frac{p}{2|\gamma|D}, \\ \mu_{\pm}^{(p)} &\approx |\gamma| \operatorname{ctanh}(|\gamma|L) \left(1 + \frac{p}{2\gamma^2 D} - \frac{pL}{|\gamma|D \sinh(2|\gamma|L)} \right) \\ &\pm |\gamma| \operatorname{ctanh}(|\gamma|L) \left(1 + \frac{1}{2 \cosh^2(|\gamma|L)} \left(\frac{p}{D\gamma^2} - \frac{pL}{|\gamma|D} \operatorname{ctanh}(|\gamma|L) \right) \right), \end{aligned}$$

so that

$$\begin{aligned} \mu_{-}^{(p)} &\approx p \frac{\tanh(\gamma L)}{2\gamma D} + O(p^2), \\ \mu_{+}^{(p)} &\approx 2\gamma \operatorname{ctanh}(\gamma L) + O(p). \end{aligned}$$

We also have

$$\begin{aligned} (\mathcal{M}_p)_{11} &\approx \gamma \operatorname{ctanh}(\gamma L) \left(1 + \frac{p}{2\gamma^2 D} - \frac{pL}{\gamma D \sinh(2\gamma L)} \right) - \gamma, \\ (\mathcal{M}_p)_{12} &\approx -\frac{\gamma}{\sinh(\gamma L)} \left(1 + \frac{p}{2\gamma^2 D} - \frac{pL \operatorname{ctanh}(\gamma L)}{2\gamma D} \right). \end{aligned}$$

In the lowest order, we also get

$$\begin{aligned} v_{-}^{(p)}(0) &\approx \frac{1}{\cosh(\gamma L) \sqrt{2(1 - \tanh(\gamma L))}} + O(p), \\ v_{-}^{(p)}(L) &\approx \sqrt{(1 - \tanh(\gamma L))/2} + O(p). \end{aligned}$$

Substituting these expressions into equation (74) for x_0 , we deduce in the leading order

$$\int_0^\infty dt e^{-pt} \mathbb{E}_0\{\ell_t\} = \frac{2\gamma D \operatorname{ctanh}(\gamma L)}{p^2} + O(1/p), \quad (\text{D.6})$$

from which equation (75) follows immediately.

Appendix E. On the numerical inversion of the Laplace transform

The inverse Laplace transform $f(t)$ of a function $\tilde{f}(p)$ can be expressed as the Bromwich integral,

$$f(t) = \frac{1}{2\pi i} \int_{\gamma} dp e^{pt} \tilde{f}(p), \quad (\text{E.1})$$

where γ is a contour from $-i\infty$ to $+i\infty$ in the complex plane that lies on the right to singularities of $\tilde{f}(p)$. In the basic Talbot algorithm, the contour γ is parameterized as

$$\gamma: \theta \rightarrow p(\theta) = \sigma + \mu(\theta \operatorname{ctan}(\theta) + \nu i\theta), \quad \theta \in (-\pi, \pi), \quad (\text{E.2})$$

with three parameters σ , μ and ν whose optimal choice depends on the function $\tilde{f}(p)$ and determines the convergence rate [86]. Using this contour, the Bromwich integral can be reduced to

$$f(t) = \frac{1}{2\pi i} \int_{-\pi}^{\pi} d\theta \frac{dp}{d\theta} e^{p(\theta)t} \tilde{f}(p(\theta)), \quad (\text{E.3})$$

and then numerically evaluated by quadratures. In this paper, we used a slightly different contour by Weideman [87]:

$$\gamma: \theta \rightarrow p(\theta) = N(0.5017\theta \operatorname{ctan}(0.6407\theta) - 0.6122 + 0.2645i\theta), \quad \theta \in (-\pi, \pi), \quad (\text{E.4})$$

where the value of N controls the accuracy of computation.

ORCID iDs

Denis S Grebenkov  <https://orcid.org/0000-0002-6273-9164>

References

- [1] Carslaw H S and Jaeger J C 1959 *Conduction of Heat in Solids* 2nd edn (Oxford: Clarendon)
- [2] Risken H 1996 *The Fokker–Planck Equation: Methods of Solution and Applications* 3rd edn (Berlin: Springer)
- [3] Gardiner C W 1983 *Handbook of Stochastic Methods for Physics, Chemistry and the Natural Sciences* (Berlin: Springer)
- [4] Redner S 2001 *A Guide to First Passage Processes* (Cambridge: Cambridge University Press)
- [5] Schuss Z 2013 *Brownian Dynamics at Boundaries and Interfaces in Physics, Chemistry and Biology* (New York: Springer)
- [6] Metzler R, Oshanin G and Redner S 2014 *First-Passage Phenomena and Their Applications* (Singapore: World Scientific)
- [7] Lindenberg K, Metzler R and Oshanin G 2019 *Chemical Kinetics: Beyond the Textbook* (Singapore: World Scientific)

- [8] Grebenkov D S 2020 *Phys. Rev. Lett.* **125** 078102
- [9] Lévy P 1965 *Processus Stochastiques et Mouvement Brownien* (Paris: Gauthier-Villard)
- [10] Itô K and McKean H P 1965 *Diffusion Processes and Their Sample Paths* (Berlin: Springer)
- [11] Freidlin M 1985 *Functional Integration and Partial Differential Equations (Annals of Mathematics Studies)* (Princeton, NJ: Princeton University Press)
- [12] Darling D A and Kac M 1957 *Trans. Am. Math. Soc.* **84** 444–58
- [13] Ray D 1963 *Illinois J. Math.* **7** 615
- [14] Knight F B 1963 *Trans. Am. Math. Soc.* **109** 56–86
- [15] Agmon N 1984 *J. Chem. Phys.* **81** 3644
- [16] Berezhkovskii A M, Zaloj V and Agmon N 1998 *Phys. Rev. E* **57** 3937
- [17] Dhar A and Majumdar S N 1999 *Phys. Rev. E* **59** 6413
- [18] Yuste S B and Acedo L 2001 *Phys. Rev. E* **64** 061107
- [19] Godrèche C and Luck J M 2001 *J. Stat. Phys.* **104** 489
- [20] Majumdar S N and Comtet A 2002 *Phys. Rev. Lett.* **89** 060601
- [21] Bénichou O, Coppey M, Klafter J, Moreau M and Oshanin G 2003 *J. Phys. A: Math. Gen.* **36** 7225–31
- [22] Condamin S, Bénichou O and Moreau M 2005 *Phys. Rev. E* **72** 016127
- [23] Condamin S, Tejedor V and Bénichou O 2007 *Phys. Rev. E* **76** 050102R
- [24] Burov S and Barkai E 2007 *Phys. Rev. Lett.* **98** 250601
- [25] Burov S and Barkai E 2011 *Phys. Rev. Lett.* **107** 170601
- [26] Collins F C and Kimball G E 1949 *J. Colloid Sci.* **4** 425
- [27] Sano H and Tachiya M 1979 *J. Chem. Phys.* **71** 1276–82
- [28] Shoup D and Szabo A 1982 *Biophys. J.* **40** 33–9
- [29] Zwanzig R 1990 *Proc. Natl Acad. Sci. USA.* **87** 5856
- [30] Sapoval B 1994 *Phys. Rev. Lett.* **73** 3314–6
- [31] Filoche M and Sapoval B 1999 *Eur. Phys. J. B* **9** 755–63
- [32] Bénichou O, Moreau M and Oshanin G 2000 *Phys. Rev. E* **61** 3388–406
- [33] Grebenkov D S, Filoche M and Sapoval B 2003 *Eur. Phys. J. B* **36** 221–31
- [34] Berezhkovskii A M, Makhnovskii Y A, Monine M I, Zitserman V Y and Shvartsman S Y 2004 *J. Chem. Phys.* **121** 11390
- [35] Grebenkov D S 2006 Partially reflected Brownian motion: a stochastic approach to transport phenomena *Focus on Probability Theory* ed L R Velle (New York: Nova Science Publishers) pp 135–69
- [36] Grebenkov D S, Filoche M and Sapoval B 2006 *Phys. Rev. E* **73** 021103
- [37] Reingruber J and Holcman D 2009 *Phys. Rev. Lett.* **103** 148102
- [38] Lawley S D and Keener J P 2015 *SIAM J. Appl. Dyn. Syst.* **14** 1845–67
- [39] Grebenkov D S and Oshanin G 2017 *Phys. Chem. Chem. Phys.* **19** 2723–39
- [40] Bernoff A J, Lindsay A E and Schmidt D D 2018 *Multiscale Model. Simul.* **16** 1411–47
- [41] Grebenkov D S 2019 *J. Chem. Phys.* **151** 104108
- [42] Mörters P and Peres Y 2010 *Brownian Motion (Cambridge Series in Statistical and Probabilistic Mathematics)* (Cambridge: Cambridge University Press)
- [43] Grebenkov D S 2007 *Phys. Rev. E* **76** 041139
- [44] Papanicolaou V G 1990 *Probab. Theory Relat. Fields* **87** 27–77
- [45] Arendt W, ter Elst A F M, Kennedy J B and Sauter M 2014 *J. Funct. Anal.* **266** 1757–86
- [46] Daners D 2014 *Positivity* **18** 235–56
- [47] ter Elst A F M and Ouhabaz E M 2014 *J. Funct. Anal.* **267** 4066–109
- [48] Behrndt J and ter Elst A F M 2015 *J. Differ. Equ.* **259** 5903–26
- [49] Arendt W and ter Elst A F M 2015 *Potential Anal.* **43** 313–40
- [50] Hassell A and Ivrii V 2017 *J. Spectr. Theory* **7** 881–905
- [51] Girouard A and Polterovich I 2017 *J. Spectr. Theory* **7** 321–59
- [52] Grebenkov D S 2019 *Phys. Rev. E* **100** 062110
- [53] Grebenkov D S 2020 *Phys. Rev. E* **102** 032125
- [54] Meerson B and Redner S 2015 *Phys. Rev. Lett.* **114** 198101
- [55] Grebenkov D S and Rupprecht J-F 2017 *J. Chem. Phys.* **146** 084106
- [56] Grebenkov D S 2021 *J. Phys. A: Math. Theor.* **54** 015003
- [57] Grebenkov D S 2020 *J. Stat. Mech.* 103205
- [58] Levitz P E, Zinsmeister M, Davidson P, Constantin D and Poncelet O 2008 *Phys. Rev. E* **78** 030102(R)

- [59] Chechkin A V, Zaid I M, Lomholt M A, Sokolov I M and Metzler R 2009 *Phys. Rev. E* **79** 040105(R)
- [60] Bénichou O, Grebenkov D, Levitz P, Loverdo C and Voituriez R 2010 *Phys. Rev. Lett.* **105** 150606
- [61] Bénichou O, Grebenkov D S, Levitz P E, Loverdo C and Voituriez R 2011 *J. Stat. Phys.* **142** 657–85
- [62] Chechkin A V, Zaid I M, Lomholt M A, Sokolov I M and Metzler R 2011 *J. Chem. Phys.* **134** 204116
- [63] Chechkin A V, Zaid I M, Lomholt M A, Sokolov I M and Metzler R 2012 *Phys. Rev. E* **86** 041101
- [64] Rupprecht J-F, Bénichou O, Grebenkov D S and Voituriez R 2012 *J. Stat. Phys.* **147** 891–918
- [65] Rupprecht J-F, Bénichou O, Grebenkov D S and Voituriez R 2012 *Phys. Rev. E* **86** 041135
- [66] Berezhkovskii A M, Dagdug L and Bezrukov S M 2015 *J. Chem. Phys.* **143** 084103
- [67] Berezhkovskii A M, Dagdug L and Bezrukov S M 2017 *J. Chem. Phys.* **147** 014103
- [68] Agmon N and Szabo A 1990 *J. Chem. Phys.* **92** 5270
- [69] Prüstel T and Tachiya M 2013 *J. Chem. Phys.* **139** 194103
- [70] Grebenkov D S 2017 *J. Chem. Phys.* **147** 134112
- [71] Lawley S D and Madrid J B 2019 *J. Chem. Phys.* **150** 214113
- [72] Reva M, DiGregorio D A and Grebenkov D S 2021 *Sci. Rep.* **11** 5377
- [73] Evans M R and Majumdar S N 2011 *Phys. Rev. Lett.* **106** 160601
- [74] Chechkin A and Sokolov I M 2018 *Phys. Rev. Lett.* **121** 050601
- [75] Evans M R and Majumdar S N 2019 *J. Phys. A: Math. Theor.* **52** 01LT01
- [76] Evans M R, Majumdar S N and Schehr G 2020 *J. Phys. A: Math. Theor.* **53** 193001
- [77] Gopalakrishnan M and Govindan B S 2011 *Bull. Math. Biol.* **73** 2483–506
- [78] Zelinski B, Müller N and Kierfeld J 2012 *Phys. Rev. E* **86** 041918
- [79] Mulder B M 2012 *Phys. Rev. E* **86** 011902
- [80] Angelani L 2017 *J. Phys. A: Math. Theor.* **50** 325601
- [81] Bressloff P C and Kim H 2019 *Phys. Rev. E* **99** 052401
- [82] Nelson E 1958 *Duke Math. J.* **25** 671–90
- [83] Szabo A, Lamm G and Weiss G H 1984 *J. Stat. Phys.* **34** 225–38
- [84] Guérin T, Dolgushev M, Bénichou O and Voituriez R 2021 *Commun. Chem.* **4** 157
- [85] Thambynayagam R K M 2011 *The Diffusion Handbook: Applied Solutions for Engineers* (New York: McGraw-Hill)
- [86] Talbot A 1979 *IMA J. Appl. Math.* **23** 97–120
- [87] Weideman J A C 2006 *SIAM J. Numer. Anal.* **44** 2342–62